Published online March 2, 2006

Interactive Effects of Elevated Carbon Dioxide and Drought on Wheat

G. W. Wall,* R. L. Garcia, B. A. Kimball, D. J. Hunsaker, P. J. Pinter, Jr., S. P. Long, C. P. Osborne, D. L. Hendrix, F. Wechsung, G. Wechsung, S. W. Leavitt, R. L. LaMorte, and S. B. Idso

ABSTRACT

Atmospheric CO_2 concentration (C_a) continues to rise. An imperative exists, therefore, to elucidate the interactive effects of elevated C_a and drought on plant water relations of wheat (*Triticum aestivum* L.). A spring wheat (cv. Yecora Rojo) crop was exposed to ambient (Control: 370 μmol mol^{-1}) and free-air CO_2 enrichment (FACE: ambient + 180 μmol mol^{-1}) under ample (Wet), and reduced (Dry), water supplies (100 and 50% replacement of evapotranspiration, respectively) over a 2-yr study. Our objective was to characterize and quantify the responses of 26 edaphic, gas exchange, water relations, carbohydrate pool dynamics, growth, and development parameters to rising C_a and drought. Increasing C_a minimized the deleterious effects of soil–water depletion by increasing drought avoidance (i.e., lower stomatal conductance and transpiration rate, and growth and development of a more robust root system) and drought tolerance (i.e., enhanced osmoregulation and adaptation of tissue) mechanisms, resulting in a 30% reduction in water stress–induced midafternoon depressions in net assimilation rate. An elevated C_a–based increase in daily and seasonal carbon gain resulted in a positive feedback between source capacity (shoots) and sink demand (roots). Devoid of a concomitant rise in global temperature resulting from the rise in C_a, improved water relations for a herbaceous, cool-season, annual, C_3 cereal monocot grass (i.e., wheat) are anticipated in a future high-CO_2 world. These findings are applicable to other graminaceous species of a similar function-type as wheat common to temperate zone grassland prairies and savannas, especially under dryland conditions.

THE atmospheric CO_2 concentration (C_a) is rising about 0.5% per annum from present day levels of approximately 370 μmol mol^{-1} and is projected to reach 500 to 1000 μmol mol^{-1} by the 21st century, depending on future emission rates (IPCC, 1996, 2001). The increase in C_a, as well as of other radiatively active gases, is predicted to cause global warming and to alter precipitation patterns (McCarthy et al., 2001). Higher levels of C_a directly affects the physiology, water relations, growth, and development of plants (Long et al., 2004; Ainsworth and Long, 2005), as do warmer temperatures and altered water supplies. In this article we focus on the effects of elevated C_a on the water relations of wheat at both ample and stress levels of soil–water supply.

Wheat is the world's foremost grain source (FAO, 1996). As such, it has been identified as a high priority for global change research (IPCC, 1996, 2001) by the Global Change and Terrestrial Ecosystems–International Geosphere–Biosphere Program (Steffen et al., 1992). Wheat, a cool-season annual monocot C_3 grass, is representative of graminaceous species common to temperate zone grassland prairies and savannas that

G.W. Wall, B.A. Kimball, D.J. Hunsaker, P.J. Pinter, Jr., R.L. LaMorte, and S.B. Idso (retired), USDA-ARS, U.S. Water Conservation Lab., 4331 E. Broadway Rd., Phoenix, AZ 85040; R.L. Garcia, LI-COR, P.O. Box 4425, Lincoln, NE 68504; S.P. Long, Univ. of Illinois, Dep. of Crop Science and Plant Biology, 1201 W. Gregory Dr., Urbana-Champaign, IL 61801; C.P. Osborne, Dep. of Animal and Plant Sciences, Univ. of Sheffield, Sheffield, S10 2TN, UK; D.L. Hendrix (retired), USDA-ARS, Western Cotton Research Lab., 4135 E. Broadway Rd., Phoenix, AZ 85040; F. Wechsung, Potsdam Institute for Climate Impact Research, P.O. Box 601203, D-14412 Potsdam, Germany; G. Wechsung, Dep. of Soil Science, Humboldt Univ. of Berlin, Invalidenstrasse 42, 10115 Berlin, Germany; and S.W. Leavitt, Lab. of Tree-Ring Research, Univ. of Arizona, Tucson, AZ, 85721. Mention of any proprietary product does not imply an endorsement or recommendation by the authors or their institution over other products not mentioned. Received 30 Mar. 2004. *Corresponding author (gwall@uswcl.ars.ag.gov).

Published in Agron. J. 98:354–381 (2006).
Agroclimatology
doi:10.2134/agronj2004.0089

677 S. Segoe Rd., Madison, WI 53711 USA

Abbreviations: A, instantaneous leaf net assimilation rate [μmol (CO_2) m^{-2} s^{-1}]; A_{max}, daily maximum leaf net assimilation rate [μmol (CO_2) m^{-2} s^{-1}]; A_N, season-long relative mean leaf net assimilation rate normalized between 0 to1 scale (i.e., $A_N = A/A_{max}$; dimensionless); A', daily integral of net leaf carbon accumulation [g (C) m^{-2} d^{-1}]; A'', seasonal integral of net leaf carbon accumulation [g (C) m^{-2} yr^{-1}]; ANOVA, analysis of variance; B_S, season-long average total shoot biomass (g m^{-2} ground area); $B_{S(max)}$ maximum season-long total shoot biomass (g m^{-2} ground area); B_R, season-long average living root biomass (g m^{-2} ground area); $B_{R(max)}$, maximum season-long living root biomass (g m^{-2} ground area); B_R/B_S, season-long living root to total shoot biomass ratio (dimensionless); CD, Control-Dry; CW, Control-Wet; C, carbon dioxide effect in ANOVA; C_a, atmospheric CO_2 concentration [μmol (CO_2) mol^{-1}]; C_i, intercellular CO_2 concentration [μmol (CO_2) mol^{-1}]; C_i/C_a, ratio of C_i to C_a (dimensionless); CHO, concentration of simple sugars (sucrose, glucose, fructose) in leaf tissue (g kg^{-1}); D, soil dehydration cycle effect in ANOVA; DAE, day after 50% emergence; E, effect in the ANOVA (i.e., Y, D, T, C, I, Z); ET, season-long average daily evapotranspiration rate (mm d^{-1}); ET_c, season-long cumulative evapotranspiration (mm); e_a, atmospheric water vapor pressure at T_a (Pa); e_s, atmospheric saturation water vapor pressure at T_a (Pa); e^*, atmospheric water vapor pressure deficit (i.e., $e^* = e_s - e_a$) at T_a (Pa); F, F statistic; FACE, free-air-CO_2-enrichment; FD, FACE-Dry; FW, FACE-Wet; Fru, concentration of fructose in leaf tissue (g kg^{-1}); g_s, stomatal conductance to water vapor [mol (H_2O) m^{-2} s^{-1}]; Glu, concentration of glucose in leaf tissue (g kg^{-1}); HMW, concentration of high molecular weight fructans in leaf tissue (g kg^{-1}); I, irrigation effect in ANOVA; IWUE (A/g_s) intrinsic water use efficiency [μmol (CO_2) mol (H_2O)$^{-1}$]; PPFD, photosynthetic photon flux density [μmol (photons) m^{-2} s^{-1}]; LMW, concentration of low molecular weight fructans in leaf tissue (g kg^{-1}); Suc, concentration of sucrose in leaf tissue (g kg^{-1}); P_α, probability of a greater F statistic by chance; S, concentration of starch in leaf tissue (g kg^{-1}); T, time of day [mid-morning (MM: 2.5 h prior to solar noon), midday (MD: solar noon), and midafternoon (MA: 2.5 h after solar noon)] effect in ANOVA; TR, leaf transpiration rate [mmol (H_2O) m^{-2} s^{-1}]; T_a, ambient air temperature inside cuvette (°C); T_l, leaf temperature inside cuvette (°C); ΔT_l, leaf – air temperature inside cuvette (°C); TNC, concentration of total nonstructural carbohydrates in leaf tissue (g kg^{-1}); WUE, (A/TR) water use efficiency [μmol (CO_2) mmol (H_2O)$^{-1}$]; Y, year effect in ANOVA; Z, canopy height effect in ANOVA; Ψ_M, soil matric potential (MPa); Ψ_W, total leaf water potential (MPa); $\Psi_{W(PB)}$, total leaf water potential measured with a pressure chamber (MPa); $\Psi_{W(PSY)}$, total leaf water potential measured with thermocouple psychrometers (MPa); Ψ_π, leaf osmotic potential (MPa); Ψ_P, leaf turgor potential (MPa); $\Delta\Psi_\pi$, rate of osmotic adjustment (dimensionless); $\Delta\Psi_P$, rate of loss of turgor (dimensionless); θ_S, volumetric soil–water content (m^3 m^{-3}).

cover a significant proportion of Earth's landmass and that make a substantial contribution to the above- and belowground global carbon balance. An imperative exists, therefore, to elucidate the effects that a future high-CO_2 world and potential changes in soil–water supply could have on edaphic, gas exchange, water relations, carbohydrate pool dynamics, growth, and development characteristics of wheat. Dissemination of such information could be of use to those individuals responsible for formulating strategies to mitigate the adverse effects of global change, while optimizing those that are beneficial (i.e., development of new cultivars with higher yields or improved grain end-use quality).

Our objective was to characterize and quantify a wheat plant's response to global change. Pursuant to this aim we elucidated the interdependency of four edaphic, nine gas exchange, four leaf tissue carbohydrate content, four water relations, and five growth parameter responses of spring wheat grown under ample and reduced soil–water content and ambient and elevated C_a levels. Specifically, we hypothesized the following:

1. An elevated C_a–based decrease in leaf stomatal conductance (g_s) will reduce depletion of volumetric soil–water content (θ_S), thereby causing less negative soil matric potential (Ψ_M).
2. Conservation of water via an elevated C_a–based reduction in g_s will enable stomata to remain open for a longer period into a drought.
3. During the diurnal period, when transpiration rates (TR) are at their maximum, elevated C_a will improve (less negative) midday total plant water potential (Ψ_W), and during the nocturnal period greater recovery in plant water status will be observed at predawn and sunset.
4. Under more severe drought conditions, elevated C_a will enhance the rate of osmotic adjustment ($\Delta\Psi_\pi$), thereby resulting in a decrease in the rate in loss of turgor ($\Delta\Psi_P$), as evidenced by leaves that maintain higher values of turgor potential (Ψ_P).
5. Under ample water supply any reduction in carbon gain will occur mostly because of nonstomatal limitations, whereas under drought conditions stomatal limitations will reduce carbon gain.
6. On a relative basis, the net gain in carbon uptake in response to elevated C_a will be proportionately greater under dry than wet.
7. Improved water relations that increase carbon gain will be evidenced by an increase in the concentration of total nonstructural carbohydrates (TNC) in source leaves.
8. Elevated C_a will foster a positive feedback relationship between aboveground source capacity (shoots) and belowground sink demand (roots), and this effect will be proportionately greater under dry than wet conditions.

To test the validity of these eight hypotheses, we characterized and quantified the effect of tissue dessication (during soil dehydration) and subsequent recovery (after soil rehydration) on a total of 26 parameters of open-field spring wheat grown in ambient air and air enriched with C_a, and under four soil dehydration–rehydration cycles over a 2-yr study.

MATERIALS AND METHODS

Site and Experimental Design

During the 1992–1993 and 1993–1994 growing seasons, two experiments were conducted to investigate the interactive effects of C_a and θ_S on spring wheat. The experiments were conducted in a 12-ha open field at the University of Arizona's Maricopa Agricultural Center, Maricopa, AZ (33.07° N lat; 111.97° W long; 361 m above sea level), located 50 km south of Phoenix, AZ. The soil was a Trix clay loam [fine-loamy, mixed (calcareous) hyperthermic Typic Torrifluvents]. Details of the field site and biological activity sampling areas (Wall and Kimball, 1993), as well as the irrigation system (Hunsaker et al., 1996), have been described previously. Except for the use of drip rather than flood irrigation, all agronomic practices were in accordance with local cultural practices.

Carbon Dioxide and Irrigation Treatment Description

The FACE approach was employed to create an elevated C_a treatment (C) (Hendrey, 1993). The FACE plots were fumigated with CO_2 24 h d^{-1} at rates required to maintain a concentration of approximately 550 μmol mol^{-1} at the center point of the plot from 50% emergence until physiological maturity (1 Jan.–16 May 1993, and 28 Dec. 1993–31 May 1994). Control plots contained a plenum and vertical vent pipes, but had no airflow and were at ambient C_a levels of approximately 370 μmol mol^{-1}. Seasonal average values of C_a were within 0.5 μmol mol^{-1} of the set point and 93% of the 1-min averages were within 10% of the set point (Hendrey, 1993) (i.e., 548 μmol mol^{-1} during the day and 598 μmol mol^{-1} at night for FACE and 363 μmol mol^{-1} during the day and 412 μmol mol^{-1} at night for Control).

Irrigation water was supplied with a subsurface drip-tape irrigation system (0.5-m tube spacing, 0.3-m emitter spacing, 0.2-m depth) as described by Hunsaker et al. (1996). Each of the main circular C plots were split into semicircular halves, with each half receiving an irrigation (I) treatment of either 100% (Wet, well-watered) or limited 50% (Dry, water-stressed) replacement of potential evapotranspiration (ET). A water balance procedure (Fox et al., 1992) was used to determine both the timing and amount of irrigated water applied to the Wet plots. An irrigation event occurred when the soil–water depletion of plant-available water in the crop root zone for Wet plots was between 30 and 40% of available. The amount of irrigated water applied to the Wet plots was then determined to replenish the root zone to field capacity (0% depletion). Because the Dry plots received only 50% as much irrigation water as the Wet plots, the depletion of water for the Dry plots was between 60 and 80% available. A preexisting crop coefficient curve developed for wheat was used to estimated crop water use that expressed the ratio of daily wheat ET to daily potential ET for a grass-reference crop. The grass-reference ET was calculated with the modified Penman equation as implemented by Doorenbos and Pruitt (1977). All meteorological data required for the modified Penman calculation was obtained from a weather station about 2 km from the field site.

For ease in applying the I treatments, the same irrigation regime was applied to the same split-plot within a C level for each replication: strip-split-plot experimental design. These C and I levels gave four treatment combinations: Control-Dry (CD); FACE-Dry (FD); Control-Wet (CW); FACE-Wet (FW).

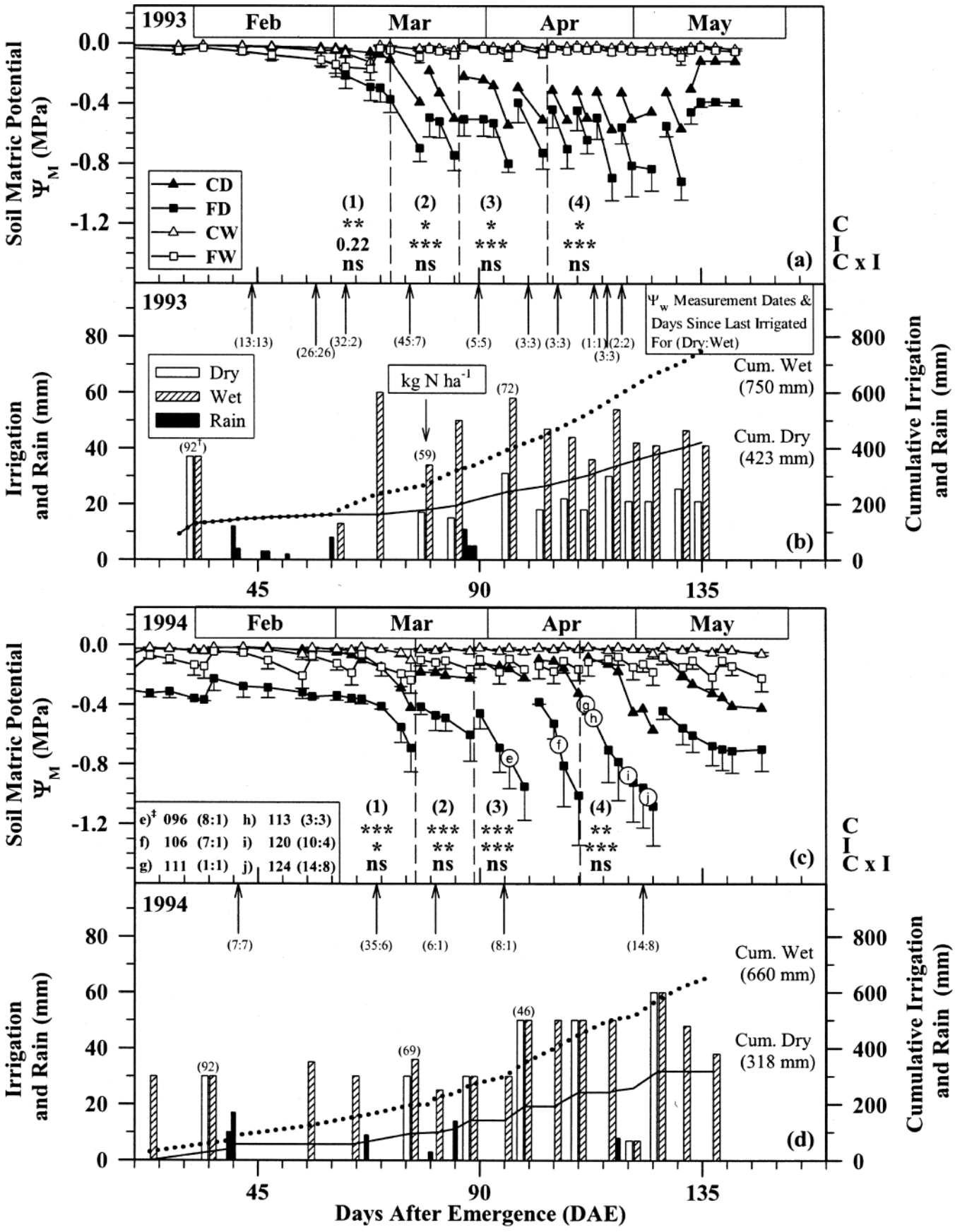

All treatments were replicated four times for a total of eight rings—four of them were active FACE rings with blowers and four of them were inactive Control rings without blowers (Pinter et al., 2000).

Crop Culture

Certified wheat seeds (cv. Yecora Rojo) were sown (John Deere Flex-Planter 71, Moline, IL) into flat beds at 0.25-m row spacings on 15 Dec. 1992 at a plant population of 130 plants m^{-2}; 50% emergence occurred on 1 Jan. 1993, and the crop was harvested 25–27 May 1993. During the second year seeds were sown at a higher plant population of 180 plants m^{-2} on 7–8 Dec. 1993; 50% emergence occurred on 28 Dec. 1993, and the crop was harvested on 1 June 1994. To germinate the seeds a drip irrigation system was used to apply 317 mm of water from 9 to 13 d after they were sown during 1993, whereas a portable sprinkler system was installed temporarily to apply a total of 30 mm of water from 6 to10 d after seeds were sown during 1994 (Fig. 1b, d). Because day after 50% emergence (DAE) corresponded with the first day of the year during this 2-yr study, hereafter DAE is equivalent to day of year.

Although the criterion for initiating an irrigation was the same for both years, irrigation application rates and frequency differed between years. During 1993, the Dry plots were irrigated with half as much water each time the Wet received an application (Fig. 1b), whereas in 1994 the Dry plots were irrigated every other Wet application date, but were given similar amounts of water as Wet (Fig. 1d). Therefore, during 1993 the irrigation regime for the Dry plots was low-volume and high-frequency, whereas in 1994 it was low-frequency and high-volume. The reason for switching to the latter strategy in the second year was to distribute the water more evenly and reduce row-to-row variation. More importantly, however, the low-frequency, high-volume irrigation strategy during 1994 provided greater soil moisture deficits over a longer period during consecutive soil dehydration cycles. Nevertheless, both strategies provided large enough differences in θ_s between Dry and Wet treatments for a comparative study (Fig. 1a, c).

Fertilizer amounts were applied so that nutrients were nonlimiting. A preplant application of granular (16–20–0) fertilizer supplied 54 kg N ha^{-1} and 29 kg P ha^{-1} in both years. Nitrogen, as urea–ammonium nitrate solution (0.32 kg N kg $fertilizer^{-1}$, Uran-32), and P, as super-phosphoric acid, fertilizer were applied through the irrigation tubes at tillering, inflorescence emergence, and anthesis (Fig. 1b, d). Total amounts of N applied were 277 and 261 kg N ha^{-1}, and of P were 44 and 29 kg P ha^{-1} during 1993 (Fig. 1b) and 1994 (Fig. 1d), respectively.

Volumetric Soil–Water Content and Evapotranspiration Rate

Measurements of θ_S were obtained in each subplot using time domain reflectometry (TDR) and neutron scattering equipment (Hydroprobe Model 503 DR, Campbell Pacific Co., Martinez, CA). Access tubes (50 mm diam. and 2.0 m long) were installed in the no-traffic section (Wall and Kimball, 1993) of each of 16 plots, before seeds were sown during 1992. The TDR measurements were taken over the 0- to 0.3-m soil depth, whereas neutron scattering measurements were taken from the 0.4- to 2.0-m depth in 0.2-m increments (Hunsaker et al., 1996). The soil-water retention characteristics for the site were estimated from data obtained from Post et al. (1988). These data were used to develop individual moisture release curves for Control and FACE plots, which were used to derive Ψ_M over a 0.9-m soil profile for each date θ_S was measured (Fig. 1a, c).

After expected root penetration had occurred to a given depth (Robertson et al., 1993a, 1993b), a stair-step model incorporated values of θ_S at consecutively deeper depths in 0.3-m intervals. By assuming negligible deep percolation, average daily ET was essentially set equal to the temporal changes in θ_S for the active root zone. Whenever irrigation or rain occurred, however, it was estimated by interpolation by using the average ET before and after the wetting event for the active root zone. Hence, θ_S and the total amount of irrigation plus rain were used to calculate ET, and therefore season-long cumulative evapotranspiration (ET_C), based on the soil–water balance method (Jensen et al., 1990) as implemented by Hunsaker et al. (1996).

Measurements of Leaf Stomatal Conductance and Net Assimilation and Transpiration Rates

Gas exchange rates were measured on randomly selected leaves with three portable closed-exchange (transient) systems with a 0.25-L transparent Plexiglas cuvette (Model LI-6200, LI-COR, Lincoln, NE). Each infrared gas analyzer was calibrated against a gravimetrically prepared mixture of CO_2 in air (±1% Primary Standard, Matheson Gas Products, Cucamonga, CA), and cuvette humidity sensors were calibrated with a dew-point generator (LI-610, LI-COR, Lincoln, NE) immediately before use. Before each measurement, the cuvette was allowed to come into equilibrium with prevailing

Fig. 1. Soil matric potential (Ψ_M) for a 0.9-m soil profile of a Trix clay loam vs. day after 50% emergence (DAE) (i.e., calendar date same as DAE) for the (a) 1993 and (c) 1994 growing seasons. Symbols in legend for panels (a) and (c) refer to Control-Dry (CD), FACE-Dry (FD), Control-Wet, and FACE-Wet (FW) treatments (Control at 370 μmol CO_2 mol^{-1} and FACE at 550 μmol CO_2 mol^{-1}; Dry at 50% and Wet at 100% replacement of evapotranspiration). Vertical dashed lines in panels (a) and (c) separate four individual soil dehydration cycles by development stages as follows: (1) seedling development, tillering, and stem elongation (DAE 1–71 during 1993; DAE 1–76 during 1994); (2) inflorescence emergence (DAE 72–85 during 1993; DAE 77–88 during 1994); (3) anthesis (DAE 86–103 during 1993; DAE 89–111 during 1994); and (4) grain filling through physiological maturity (DAE 104–136 during 1993; DAE 112–137 during 1994). Symbols in legend given in panel (b) refer to drip-tape irrigation for Dry and Wet treatments, rainfall amounts, and N fertilizer application dates during (b) 1993 and (d) 1994. † Amount of fertilizer (kg N ha^{-1}) applied is given in parenthesis above irrigation histograms at tillering, inflorescence emergence, and anthesis for (b) 1993 and (d) 1994. Cumulative distribution curves (Cum.) denoting the amount of water (drip-tape irrigation + rainfall) given by right-most *y* intercept for Dry and Wet treatments in panels (b) and (d). Onset of the differential irrigation denoted by separation in Cum. curves on 1 Mar. 1993 (DAE 60) in panel (b) and 20 Jan. 1994 (DAE 20) in panel (d). Up-pointing arrows in panels (b) and (d) denote DAE when gas exchange, water relation, and leaf tissue carbohydrate concentration measurements were measured, whereas parenthesis below up-pointing arrows denote number of days between measurement dates and the last irrigated for (Dry:Wet) treatments. ‡ Letters e through j in legend of panel (c) denote DAE and number of days between measurement dates and last irrigated for (Dry:Wet) treatments during the third (e, f) and fourth (g, h, i, and j) soil dehydration cycles when standard thermocouple psychometric techniques were employed to measure leaf total water and osmotic potentials during 1994. Given on the right-most *y* axis are the sources of variance in ANOVA, which include carbon dioxide (C) for main plot, irrigation (I) for split-plot, and $C \times I$ interaction effects in a strip-split-plot experimental design. Significance effects given within soil dehydration cycle as *, **, *, and ns for $P_\alpha \leq 0.05$, $P_\alpha \leq 0.01$, $P_\alpha \leq 0.001$, and not significant, respectively (ne for effect not estimated); actual probability of a greater *F* statistic by chance reported if $P_\alpha \geq 0.10$ and $P_\alpha \leq 0.25$ § $P_\alpha \leq 0.10$. Each mean datum was derived from four replications (i.e., means based on $n = 4$, SE of replication means based on $n = 4$).**

air temperature and relative humidity. As described previously by Wall et al. (2000), dawn to dusk measurements of g_s, and net assimilation (A) and transpiration (TR) rates were made on the central portion of fully expanded (ligule emerged) upper-canopy sunlit leaves, begun at a cuvette CO_2 concentration of 370 ± 35 or 550 ± 35 μmol mol^{-1} for Control and FACE, respectively. One leaf per row from each of five different rows (repeated measures) was randomly selected for measurement. The leaf cuvette was held in the horizontal position and caution was used not to shade any portion of the leaf. Because three separate portable closed-exchange systems were used, three replications could be measured simultaneously within 60 min at 2-h intervals, thereby minimizing variation in gas exchange measurements due to diurnal changes in meteorological conditions, particularly incident photon flux density (PPFD: μmol photons m^{-2} s^{-1}), air temperature (T_a), and water vapor pressure deficit (e^*) (i.e., $e^* = e_s - e_a$). Three observations were recorded, but the first 10-s measurement interval was discarded from the statistical analysis because C_a in the assimilation chamber was unstable during that period.

Each gas exchange system made direct measurements of C_a, atmospheric water vapor pressure (e_a), leaf temperature (T_l), T_a, and incident PPFD normal to the leaf surface. We calculated leaf A, g_s, TR, saturation water vapor pressure (e_s), e^*, internal CO_2 concentration (C_i) and the ratio of C_i to C_a (C_i/C_a) as suggested by LI-COR (1990) following equations of von Caemmerer and Farquhar (1981). A value for water use efficiency (WUE) and intrinsic water use efficiency (IWUE) was derived as the ratio of A to TR and A to g_s, respectively, whereas the difference between T_l and T_a was used to derive the leaf minus air temperature (ΔT_l). Phenological development (average numerical decimal code across all treatments) was used to group values of the 26 response parameters by distinctive development stages (Zadoks et al., 1974) as follows; inflorescence emergence until hard dough (DAE 75, 89, 99, 105, and 118; Zadoks 50–88) during 1993; tillering until soft dough (DAE 41, 69, 81, 95, and 123; Zadoks 24–84) during 1994. To investigate the effect of the lack of blowers in the Control plots (Pinter et al., 2000), during 1994 additional midday measurements of gas exchange parameters (i.e., g_s, A, TR, T_l, ΔT, C_i, C_i/C_a) were taken on DAE 116, 119, 126, 131, 133, and 137 from grain filling until physiological maturity (Zadoks 84.1–87.8).

The daily accumulation of carbon (A') was derived by integrating the area under each dawn to dusk net carbon uptake curve. Dawn and dusk times in Mountain Standard Time (MST) were obtained from standard astronomical tables for Maricopa, AZ, and served as a zero response point for the purpose of integration. The seasonal accumulation of net carbon uptake (A'') was derived by integrating the area under each daily carbon uptake curve from 50% emergence until canopy senescence reduced fractional absorption of PPFD to 25% using a trapezoidal integration routine (Area.xfm, Sigma Plot, v. 4.01, SPSS, Chicago, IL).

Analysis of Leaf Total Nonstructural Carbohydrate Concentration

Ten uppermost fully expanded (i.e., ligule emerged) sunlit leaves were randomly selected every 2 h (as many as eight sample intervals) from dawn to dusk. Sampling dates corresponded with the development of leaf number five through eight and the flag leaf. At anthesis on DAE 81 during 1994, after the canopy had reached its maximum height, a whole-canopy leaf profile was sampled from the flag (top of the canopy) through the flag-4 leaf (lower photosynthetically active leaf at the bottom of the canopy) on an individual culm for each of 10 culms. All leaf samples for each treatment were pooled and kept on dry ice for up to 10 h until they were transported to the laboratory. Leaves were kept overnight on dry ice in a cold storage facility maintained at 10°C. The following day the leaf samples were freeze-dried, ground through a 0.4-mm mesh in a Wiley Mill, and quickly transferred to tightly stoppered glass vials that were stored at room temperature.

The TNC, comprised of simple sugars such as glucose (Glu), fructose (Fru), and sucrose (Suc), and complex carbohydrates such as low (LMW) and high (HMW) molecular weight fructans and starch (S), were determined using a microplate assay methodology as described elsewhere (Hendrix and Peelen, 1987; Hendrix, 1993).

Measurements of Total Leaf Water Potential with a Pressure Chamber

Blades of uppermost fully expanded sunlit leaves were excised approximately 5 mm apical to the leaf collar and sealed in a plastic bag containing a damp paper towel. Plastic bags containing excised leaves were then stored in an insulated container containing ice. No direct contact occurred between the ice and leaf samples. Values of Ψ_W were measured with a pressure chamber (bomb) ($\Psi_{W(PB)}$) (Scholander et al., 1965) (Model 3000, Soil Moisture Equipment Corp, Santa Barbara, CA). This protocol has given reliable results as long as particular precautions are taken to minimize error due to rapid water loss (Turner and Long, 1990).

Measurements of Total Leaf Water and Osmotic Potentials with Thermocouple Psychrometers

Measurements of thermocouple psychrometers-based total leaf water ($\Psi_{W(PSY)}$) and osmotic Ψ_π potentials were made using standard psychrometric techniques (Brown and Collins, 1980; Walker et al., 1983; Briscoe, 1984). A leaf sample approximately 50 mm long was rapidly excised from the central section of the uppermost fully expanded sunlit leaf (excluding the midrib), rolled, and inserted into the sample chamber and sealed within 15 s. Surgical gloves were worn to minimize contamination of the sample. Psychrometer chambers containing an excised leaf were placed in an insulated isothermal cooler at the field site and transported to a temperature-controlled room maintained at 25°C within 2 to 4 h. The $\Psi_{W(PSY)}$ was measured when thermal and vapor pressure equilibrium had been established (within 4 h). The sample chambers were then frozen in liquid N_2 for 3 min and thawed. Measurements of Ψ_π were obtained after re-establishment of thermal and vapor pressure equilibrium (within 2 h). Measurements of $\Psi_{W(PSY)}$ and Ψ_π were taken at midday from anthesis through grain filling, up to soft dough, which corresponds with the third (e:96 and f:106) and fourth (g:111, h:113, i:120, and j:124) soil dehydration cycles during 1994 (letters in circles correspond with DAE illustrated for FD treatment in Fig. 1c). Both midday and midafternoon psychrometric measurements were taken on DAE 124. Values of turgor potential (Ψ_P) were derived from $\Psi_{W(PSY)}$ and Ψ_π (i.e., $\Psi_P = \Psi_{W(PSY)} - \Psi_\pi$; Kirkham, 1990). No attempt was made to correct the psychrometric obtained measurements of Ψ_π for apoplastic dilution of the symplast (Campbell et al., 1979) or starch hydrolysis (Bennett et al., 1986).

Two types of leaf in situ thermocouple psychrometers were used in combination with their associated stainless steel sampling chambers; 48 of them were Model 84-3vC psychrometers (J.R.D. Merrill Specialty Equipment, Logan, UT), and 36 of them were Model C-30 psychrometers (Wescor, Logan, UT).

Root and Shoot Growth

The seasonal average (B_R) and maximum ($B_{R(max)}$) living root biomass (excluding crown tissue) in a 1-m soil profile was ob-

Table 1. ANOVA for CO_2 [*C*: Control (370 μmol mol^{-1}); FACE (550 μmol mol^{-1})], irrigation [*I*: Dry (50%); Wet (100% replacement of evapotranspiration)], Year (*Y*: 1993, 1994), soil dehydration cycle [*D*: first (tillering-stem elongation), second (inflorescence emergence), third (anthesis), fourth (grain filling)], and time of day [(*T*: midmorning (MM), midday (MD), and midafternoon (MA)] effects on four edaphic, nine gas exchange, four water relation, four leaf tissue concentration of carbohydrates, and five growth parameters for field-grown spring wheat [*Triticum aestivum* (L.) cv. Yecora Rojo] during the 1993 and 1994 growing seasons.

		Edaphic				Gas exchange									Water relation				Carbohydrate				Growth				
Source†	df‡	θ_S	Ψ_M	ET	ET_C	g_s	A	TR	T_l	ΔT	WUE	IWUE	C_i	C_i/C_a	$\Psi_{W(PB)}$	$\Psi_{W(PSY)}$	Ψ_π	Ψ_P	CHO	FRU	S	TNC	B_S	B_R	B_R/B_S	$B_{R(max)}$	$B_{S(max)}$
C	1	ns	*	ns	ns	**	**	**	**	**	**	***	**	**	***	ns	ns	ns	**	***	**	**	**	***	ns	§	§
I	1	**	**	***	**	**	**	*	**	**	*	*	**	*	***	**	**	ns	**	***	***	**	§	ns	*	0.18	**
C × *I*	1	**	§	0.19	§	**	ns	*	ns	0.24	ns	**	ns	§	*	ns	ns	0.15	***	**	**	***	ns	ns	ns	ns	ns
Y	1	ns	*	ns	ns	*	ns	§	*	**	*	*	*	*	§				***	ns	**	***	***	***	ns	**	ns
Y × *C*	1	**	***	ns	ns	ns	ns	ns	ns	ns	ns	§	*	ns	ns				**	ns	**	ns	***	**	ns	§	ns
Y × *I*	1	ns	ns	**	*	ns	**	§	**	ns	ns	§	*	§	§				***	***	*	**	***	ns	ns	ns	ns
Y × *C* × *I*	1	***	ns	ns	ns	0.11	0.20	0.12	ns	ns	ns	ns	ns	ns	**				*	ns	ns	*	ns	ns	ns	ns	§
D	3	***	**	***		**	**	ns	**	ns	**	**	**	**	***	**	*	***	***	***	***	***	§	***	***		
D × *C*	3	ns	ns	ns		ns	**	ns	ns	ns	0.11	0.15	**	**	*	ns	ns	§	**	**	***	***	ns	*	ns		
D × *I*	3	***	**	***		**	**	**	**	**	**	ns	**	0.12	**	§	ns	0.14	§	**	***	**	***	ns	ns		
D × *C* × *I*	3	ns	ns	ns		ns	*	ns	ns	ns	ns	ns	ns	ns	*	ns	ns	0.12	**	**	**	**	ns	ns	ns		
D × *Y*	3	***	*	***		**	**	*	*	*	**	§	**	**	**				**	***	***	***	§	***	***		
D × *Y* × *C*	3	ns	ns	ns		ns	ns	ns	ns	ns	ns	ns	0.18	ns	§				**	ns	**	**	ns	0.17	ns		
D × *Y* × *I*	3	**	**	ns		**	**	§	§	ns	**	0.22	0.19	0.15	0.14				§	**	***	**	*	ns	ns		
D × *Y* × *C* × *I*	3	0.16	ns	ns		ns	ns	ns	ns	ns	ns	ns	ns	ns	ns				**	0.19	**	0.11	ns	0.15	ns		
T	2					ns	**	***	**	**	**	***	**	**	***				***	***	***	***					
T × *C*	2					ns	0.21	ns	ns	ns	0.19	ns	0.21	ns	0.22				§	*	***	**					
T × *I*	2					0.15	*	*	ns	ns	ns	ns	ns	ns	**				§	*	***	*					
T × *C* × *I*	2					§	**	ns	0.19	0.18	ns	ns	ns	ns	0.17				§	*	*	**					
T × *Y*	2					ns	**	***	**	0.13	§	ns	**	§	*				***	0.23	***	0.19					
T × *Y* × *C*	2					ns	ns	0.19	0.14	ns	0.23	ns	ns	ns	0.19				ns	ns	**	ns					
T × *Y* × *I*	2					**	*	***	0.11	**	*	**	ns	ns	**				§	0.12	***	*					
T × *Y* × *C* × *I*	2					ns	ns	ns	ns	*	ns	ns	ns	ns	ns				§	ns	*	§					
T × *D*	6					**	ns	**	**	§	0.25	*	**	**	***				***	***	***	***					
T × *D* × *C*	6					ns	0.12	ns	ns	ns	ns	ns	0.24	ns	ns				ns	0.11	***	*					
T × *D* × *I*	6					ns	0.14	ns	**	ns	ns	ns	ns	ns	*				*	*	**	ns					
T × *D* × *C* × *I*	6					ns	ns	ns	ns	ns	ns	ns	ns	ns	0.23				ns	ns	ns	ns					
T × *Y* × *D*	6					**	§	**	**	0.19	ns	*	**	**	**				***	*	***	***					
T × *Y* × *D* × *C*	6					ns	ns	ns	ns	0.13	ns	ns	ns	ns	ns				*	ns	ns	*					
T × *Y* × *D* × *I*	6					§	§	0.15	§	0.13	*	*	0.18	*	*				*	*	**	0.13					
T × *Y* × *D* × *C* × *I*	6					ns	ns	ns	ns	0.14	ns	ns	ns	ns	ns				ns	ns	ns	ns					

The symbols *, **, ***, and ns are used to show significance at $P_\alpha \leq 0.05$, $P_\alpha \leq 0.01$, $P_\alpha \leq 0.001$, and not significant, respectively; actual probability of a greater *F* value by chance reported if $P_\alpha > 0.10$ and $P_\alpha \leq 0.25$.

† Source of variance in ANOVA (error term) include *C*, *I*, *D*, *Y*, and *T* effects: *C* (*R* × *C*), *I* (*R* × *I*), *C* × *I* (*R* × *C* × *I*), *Y* (*R* × *Y*), *Y* × *C* (*R* × *Y* × *C*), *Y* × *I* (*R* × *Y* × *I*), *Y* × *C* × *I* (*R* × *Y* × *C* × *I*), *D* (*R* × *D*), *D* × *C* (*R* × *D* × *C*), *D* × *I* (*R* × *D* × *I*), *D* × *C* × *I* (*R* × *D* × *C* × *I*), *Y* × *D* (*R* × *Y* × *D*), *Y* × *D* × *C* (*R* × *Y* × *D* × *C*), *Y* × *D* × *I* (*R* × *Y* × *D* × *I*), *Y* × *D* × *C* × *I* (*R* × *Y* × *D* × *C* × *I*), *T* (*R* × *T*), *T* × *C* (*R* × *T* × *C*), *T* × *I* (*R* × *T* × *I*), *T* × *C* × *I* (*R* × *T* × *C* × *I*), *Y* × *T* (*R* × *Y* × *T*), *Y* × *T* × *C* (*R* × *Y* × *T* × *C*), *Y* × *T* × *I* (*R* × *Y* × *T* × *I*), *Y* × *T* × *C* × *I* (*R* × *Y* × *T* × *C* × *I*), *D* × *T* (*R* × *D* × *T*), *D* × *T* × *C* (*R* × *D* × *T* × *C*), *D* × *T* × *I* (*R* × *D* × *T* × *I*), *D* × *T* × *C* × *I* (*R* × *D* × *T* × *C* × *I*), *Y* × *D* × *T* (*R* × *Y* × *D* × *T*), *Y* × *D* × *T* × *C* (*R* × *Y* × *D* × *T* × *C*), *Y* × *D* × *T* × *I* (*R* × *Y* × *D* × *T* × *I*), *Y* × *D* × *T* × *C* × *I* (*R* × *Y* × *D* × *T* × *C* × *I*).

‡ df, degrees of freedom; θ_S, volumetric soil–water content; Ψ_M, soil matric potential; ET, evapotranspiration rate; ET_c, cumulative evapotranspiration; g_s, stomatal conductance to water vapor; *A*, net assimilation rate; WUE, water use efficiency (*A*/TR); IWUE, intrinsic water use efficiency (A/g_s); TR, transpiration rate; T_l, leaf temperature; ΔT, leaf minus air temperature; C_i, internal CO_2 concentration in mesophyll tissue; C_i/C_a, ratio of C_i to atmospheric CO_2 concentration (C_a); $\Psi_{W(PB)}$, total plant water potential measured with a pressure chamber (bomb); $\Psi_{W(PSY)}$, total plant water potential measured with thermocouple psychrometers; Ψ_π, osmotic potential measured with thermocouple psychrometers; Ψ_P, turgor potential (i.e., $\Psi_P = \Psi_{W(PSY)} - \Psi_\pi$); CHO, leaf tissue concentration of simple sugars (glucose, fructose, sucrose); FRU, leaf tissue concentration of complex carbohydrates (low and high molecular weight fructans); *S*, leaf tissue concentration of starch; TNC, leaf tissue concentration of total nonstructural carbohydrates; B_S, season-long average total shoot biomass; B_R, season-long average living root biomass; B_R/B_S, root to shoot ratio; $B_{R(max)}$, season-long maximum living root biomass; $B_{S(max)}$, season-long maximum total shoot biomass. ANOVAs on g_s, WUE, IWUE, C_i/C_a, and B_R/B_S performed on $Log_{(10)}$ transformation.

§ $P_\alpha \leq 0.10$.

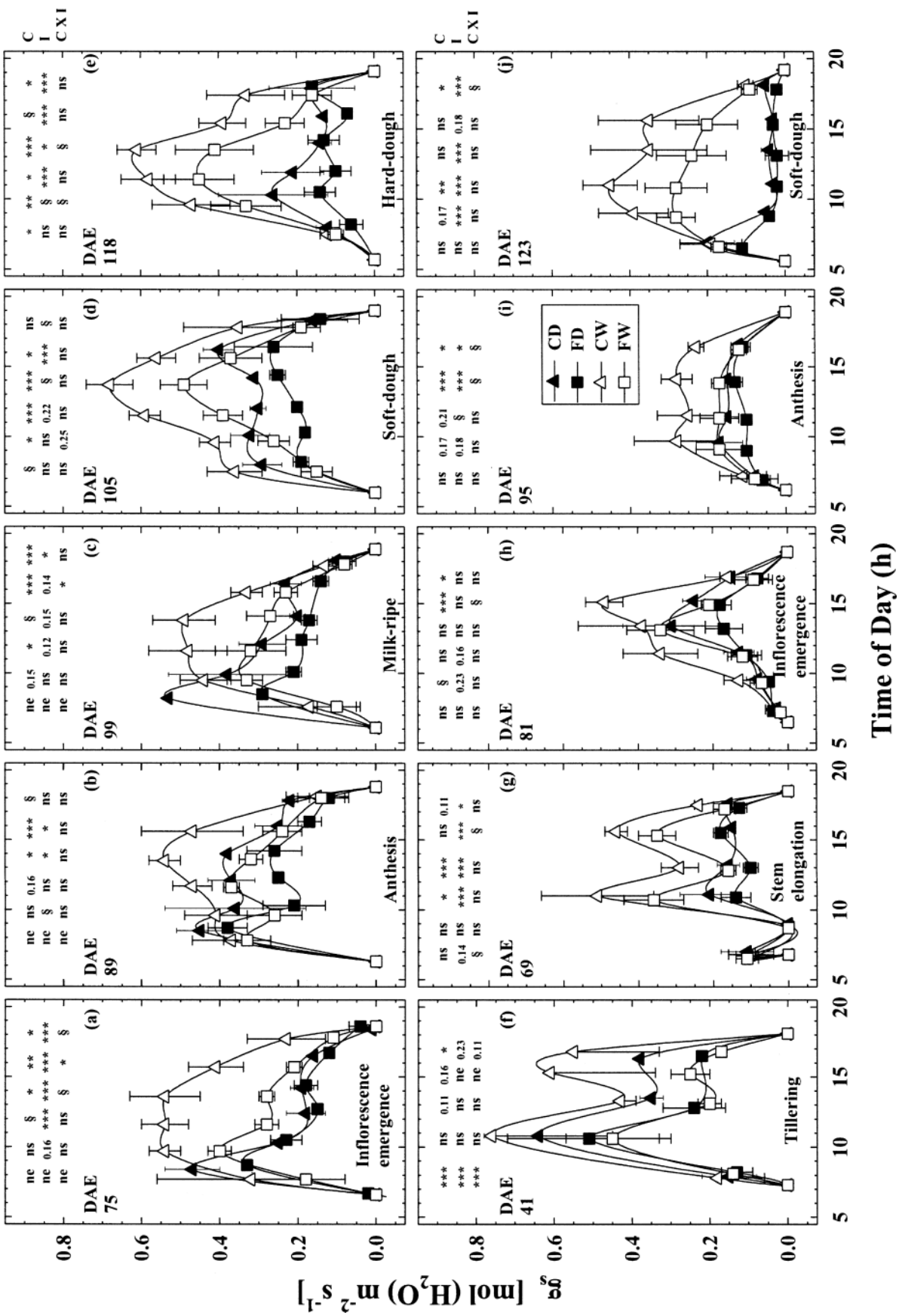

tained from two in-row and one inter-row root cores (86 mm, i.d.) using a gas-driven soil core device (Eijkelkamp Agrisearch Equipment, Cobra Model 248, Sweden). Cores were extracted with a portable lever system to minimize mechanical damage to adjacent sampling areas. Following extraction, all individual cores were placed in a −14°C freezer within 4 h of sampling. Root and organic debris material from each core was elutriated (Smucker et al., 1982) from the soil with a modified hydropneumatic elutriation system (Wall, 2000). Live roots were separated from organic debris material manually (intact, white-colored roots). The total shoot biomass (B_S) above each root core (i.e., aboveground green and brown leaves, sheaths, culms, and ears and belowground crown tissue) was also collected. From these data the seasonal maximum shoot biomass ($B_{S(max)}$) was obtained. Both B_R and B_S material were oven-dried at 68°C for 48 h, desiccator cooled, and weighed. Lastly, the root/shoot ratio (B_R/B_S) was derived from values of B_R and B_S.

Statistical Analysis

Data were analyzed as a strip-split-plot design using the SAS Mixed Procedure (Littell et al., 1996) for the ANOVAs with *C* as the main plot and *I* as the strip-split plot (Wall and Kimball, 1993). A third factor in the ANOVA was soil dehydration cycles (*D*). As many as nine and six soil dehydration cycles occurred in the Dry plots during 1993 and 1994, respectively (Fig. 1a, c), whereas the Wet plots remained hydrated throughout the experiment. Nevertheless, to synchronize development stages and soil dehydration cycles between years, both Dry and Wet plots were reclassified into two separate soil dehydration cycles during vegetative and reproductive development, respectively. The *D* effect was treated as a repeated measure specifying first order, autoregression correlation for the covariance structure. Time of day (*T*) was treated as a fourth factor in the ANOVA [MM: midmorning (2.5 h before solar noon); MD: midday (solar noon); MA: midafternoon (2.5 h after solar noon)]. A fifth factor in the ANOVA was year (*Y*). To determine the effect of leaf position (*Z*) on TNC levels, a three-way ANOVA (i.e., *Z*, *C*, *I*) was performed.

To avoid pseudo-replication, all ANOVAs were performed on replication means. Effects (*E*) (i.e., *Y*, *D*, *T*, *C*, *I*, *Z*) declared "significant" in the text have P_α values ≤ 0.05 unless stated otherwise. Tests for homogeneity of variance and subsequent data transformation were performed whenever appropriate before any ANOVA (Box et al., 1978). A covariant analysis ($\Psi_{W(PSY)}$ as the covariant) was used to determine the *C* effect on $\Delta\Psi_\pi$ and $\Delta\Psi_P$.

RESULTS AND DISCUSSION

Atmospheric Conditions

Despite a slight difference in rainfall events between years (Fig. 1b, d), climatic conditions (i.e., T_a, PPFD, and e^*) in this semiarid desert region were similar between 1993 and 1994. Briefly, all measurement days had predominantly clear skies (Kimball et al., 1995; Garcia et al., 1998). During both growing seasons, maximum hourly and total solar radiation increased from 2.2 to 3.6 MJ m^{-2} h^{-1} and 14 to 28 MJ m^{-2} d^{-1}, respectively, from January through May. Consequently, a corresponding increase in maximum T_a from 18 to 34°C occurred. An increase in the evaporative demand imposed on the crop was evident from the increase in midday e^*, which ranged from 1.0 kPa at tillering to just under 5 kPa at hard dough for both years. Although peak PPFD, in excess of 2000 μmol (photons) m^{-2} s^{-1}, occurred at solar noon, diurnal peaks in T_a and e^* occurred at mid- to late afternoon, a period when any water stress symptoms are usually at their peak. Nevertheless, temporal trends in accumulated thermal time and ontogeny of the crop were similar between years (Pinter et al., 1996).

Analysis of Variance

Overall, *C*, *I*, and $C \times I$ interactive effects were consistent across *Y*, *D*, and *T* effects (Table 1). The *I* effect predominated over the *C* effect. Significance $C \times I$ interaction effects increased in both frequency and level of significance (lower P_α value) as θ_S became depleted. This occurred mostly because of a proportionately greater disparity in the *C* effect under Dry compared with that under Wet. Significant *Y* effects occurred primarily because the low-volume, high-frequency irrigation regime caused only mild water stress during 1993, whereas the high-volume, low-frequency irrigation regime caused more severe water stress during 1994 (Fig. 1a, c). The *D* effect was insignificant during vegetative development (first and second soil dehydration cycles), but both the frequency and level of significance of the *D* effect increased during reproductive development (third and fourth soil dehydration cycles) (Fig. 1a, c). Significant *T* effects occurred primarily because of a greater responsiveness of parameters at MA (a period when drought stress is usually at its diurnal peak) compared with either MM or MD.

Higher-order interactive effects followed a consistent pattern. They occurred mostly because the *C*, *I*, and $C \times I$ interactive effects were more prevalent at MA compared with either MM or MD, during the fourth soil dehydration cycle compared with the prior three, and when soil moisture deficits were greater during 1994 compared with 1993. Higher-order interactions were most prevalent and were more significant for physiological parameters such as g_s (Fig. 2 and 7; Table 1), Ψ_W (Fig. 3, 4, and 5; Table 1), *A* (Fig. 6 and 7; Table 1), and particularly TNC (Fig. 8 and 9), whereas they were less prevalent and less significant for edaphic (Fig. 1; Table 1) and growth (Fig. 13; Table 1) parameters.

Fig. 2. Dawn to dusk trends in mean stomatal conductance to water vapor (g_s) of fully expanded sunlit spring wheat leaves for day after 50% emergence (DAE) and development stages given for 5 d during the (a–e) 1993 and (f–j) 1994 growing seasons. Typical values of photosynthetic photon flux density, air temperature, and vapor pressure deficit for this semiarid desert region, for DAE 75–118 during (a–e) 1993, have been reported elsewhere (Garcia et al., 1998). Symbols in legend and sources of variance and results from ANOVA same as described in Fig. 1. Each mean datum was derived from five leaves across two observations (repeated measures), made within a 60- to 90-min period (U.S. Mountain Standard Time), across two replications for Dry or four replications for Wet during 1993 and three replications for both Dry and Wet during 1994 (i.e., means based on $n = 20$ for Dry and $n = 40$ for Wet during 1993, and means based on $n = 30$ for both Dry and Wet during 1994). Vertical bars are 1 SE of replication means (i.e., based on n =?= 2 for Dry and $n = 4$ for Wet during 1993 and $n = 3$ for both Dry and Wet during 1994). The above illustration was derived from measurements of as many as 3540 leaves.

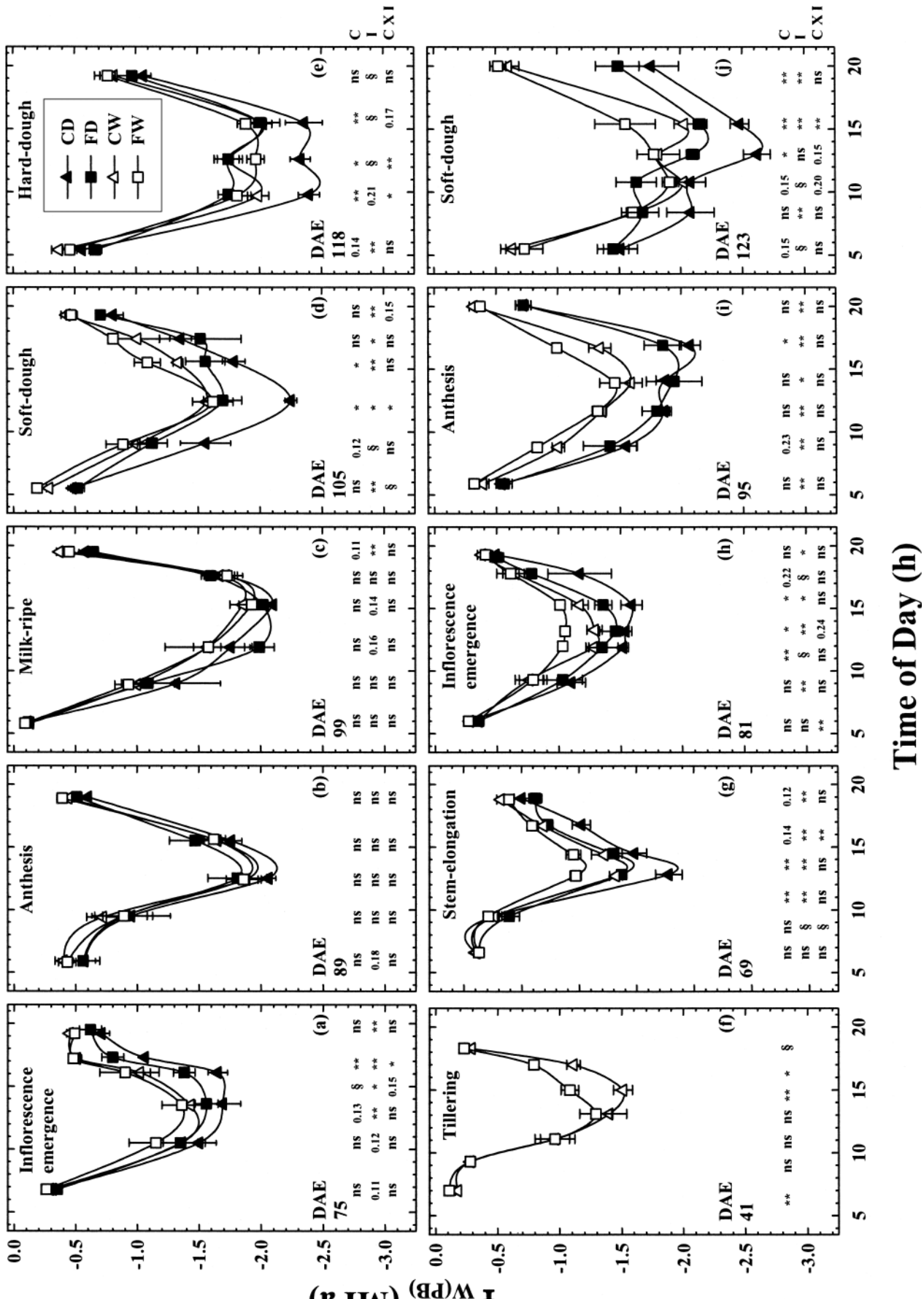

Edaphic Characteristics

Hypothesis 1: An elevated C_a–based decrease in g_s will reduce depletion of θ_S, thereby causing less negative Ψ_M

Across a 0.90-m soil profile, the θ_S was maintained at a soil–water depletion of between 30 and 40% of available water in the Wet plots, whereas it was reduced to as low as 60 to 80% of available water for the Dry plots (Hunsaker et al., 1996). Over the 2-yr study, rainfall amounts were nominal (Fig. 1b, d); therefore, values of θ_S in the Dry plots became progressively lower with consecutive soil dehydration cycles (Fig. 1a, c). Although the high-volume, low-frequency irrigation strategy enabled greater soil dehydration during 1994 (Fig. 1c, d) than the low-volume, high-frequency one did during 1993 (Fig. 1a, b), these irrigation strategies provided large enough differences in θ_S between Dry and Wet treatments for a comparative study.

Since θ_S was used to derive Ψ_M, patterns in *Y*, *D*, *C*, and *I* and their interaction effects were similar (Table 1). For well-watered wheat (Wet), Ψ_M remained relatively constant at field capacity (i.e., $\Psi_M \geq -0.03$ MPa) throughout the season (Fig. 1a, c). Notwithstanding, because of a slight reduction in whole-canopy ET (Table 2), presumably because of an elevated C_a–induced reduction in g_s (Fig. 2; Table 3), a slight reduction in soil–water depletion was observed for well-watered wheat grown in elevated C_a. The mitigating effect of elevated C_a in conserving θ_S via a reduction in g_s, however, can be counterbalanced by the relatively greater stimulation of elevated C_a in increasing root/shoot biomass (Fig. 13) and subsequent leaf area (Kimball et al., 1995; Samarakoon and Gifford, 1995; Pinter et al., 1996). Under ample water supply, therefore, elevated C_a had only a nominal effect on soil–water depletion. Nevertheless, Ψ_M was not sensitive enough to detect these minor differences in soil–water depletion, whereas the soil–water (Hunsaker et al., 1996) and energy (Kimball et al., 1995) balance methods were. Therefore, under ample water supply we accept Hypothesis 1 for θ_S, but reject it for Ψ_M.

Under Dry conditions, values of Ψ_M were as negative as −0.91 MPa for FD, but only reached −0.27 MPa for CD (Fig. 1c). The soil–water balance analysis demonstrated that wheat grown under elevated C_a and ample water supply (Wet) had a 5% reduction in seasonal ET_c compared with Control. In contrast, under limited water supply (Dry) an increase of 5 and 0.9% in ET_c occurred compared with Control under mild (1993) and more severe drought (1994) conditions, respectively (Hunsaker et al., 1996). This resulted in greater soil–water depletion when water was limited compared with when it was abundant, suggesting that the more robust root system, particularly fine roots, under FACE (Fig. 13a, b) (Wechsung et al., 1995, 1999) was able to extract more water from the soil. Under limited water supply, therefore, elevated C_a caused lower θ_S, hence more negative Ψ_M (Fig. 1a, c), particularly when drought conditions were the most severe during the fourth soil dehydration cycle at grain filling during 1994 (Fig. 1c). Hence, under reduced water supply, we reject Hypothesis 1 for both θ_S and Ψ_M.

Water Vapor Exchange Rates

Hypothesis 2: Conservation of water via an elevated C_a–based reduction in g_s will enable stomata to remain open for a longer period into a drought

The overall treatment response ranking for g_s was CW > FW ≅ CD > FD (Fig. 2). Across most of the sunlit period an approximately 180 μmol mol^{-1} increase in C_a reduced g_s for well-watered wheat by 33%, regardless of time of day (Fig. 2; Tables 1, 3). Furthermore, any differences in g_s resulted from a decrease in stomatal aperture, rather than stomatal density (Estiarte et al., 1994). Morison (1993, 1998) reported that a C_a as high as twice (i.e., 700 μmol CO_2 mol^{-1}) that in the present atmosphere generally resulted in a reduction in g_s of well-watered wheat at midday by about 40% (±5%). The elevated CO_2–based reduction in g_s across the sunlit period for well-watered wheat reported herein was consistent with a 20% lower TR measured in a leaf cuvette (Table 3), and with companion studies that showed a 7 to 23% lower TR obtained from stem flow gauges (Senock et al., 1996), an 8% lower latent heat flux derived from energy balance measurements (Kimball et al., 1995, 1999), a 5% lower rate of θ_S extraction derived through a soil–water balance technique (Hunsaker et al., 1996), lower apparent root hydraulic conductivity (Wall, unpublished data, 1994), a 1.5°C increase in individual leaf temperature measured in a cuvette (Table 3), a 0.6°C increase in daytime canopy surface temperatures (Kimball et al., 1995), and improved (less negative) $\Psi_{W(PB)}$ of 0.04 MPa (3%) (Fig. 3–5; Tables 1, 3).

Under water stress, g_s was reduced by as much as 70% (Fig. 2; Tables 1, 3). Furthermore, under drought conditions, the effect of elevated C_a on g_s was dependent on *T* (Fig. 2; Tables 1, 3) because g_s was reduced by an insignificant 2% at MM and MD, but it was reduced by a significant 25% at MA (Fig. 2). This elevated C_a–based reduction in g_s across the sunlit period for water-stressed wheat lowered TR measured in a leaf cuvette by 29% (Table 3) and improved (less negative) $\Psi_{W(PB)}$ by 0.16 MPa (9%) (Fig. 3–5; Tables 1, 3). Significant $C \times I$ interaction effects occurred because of a greater disparity in TR between FD and CD than between FW and CW (Tables 1, 3). Under drought conditions and ambient C_a levels, the more negative values of $\Psi_{W(PB)}$ induced a reduction in stomatal aperture. But, under elevated C_a, less negative values of $\Psi_{W(PB)}$ enabled less of

Fig. 3. Predawn to sunset trends in mean total leaf water potential measured with a pressure chamber ($\Psi_{W(PB)}$) of expanded sunlit spring wheat leaves for 50% day after emergence (DAE) and development stages given for 5 d during the (a–e) 1993 and (f–j) 1994 growing seasons. Symbols in legend, sources of variance, and results from ANOVA same as described in Fig. 1. Each mean datum was derived from three to four subsamples for four replications (i.e., means based on $n = 12$ or $n = 16$). Vertical bars are 1 SE of replication means (i.e., $n = 4$). The above illustration was derived from measurements from as many as 3392 leaves.

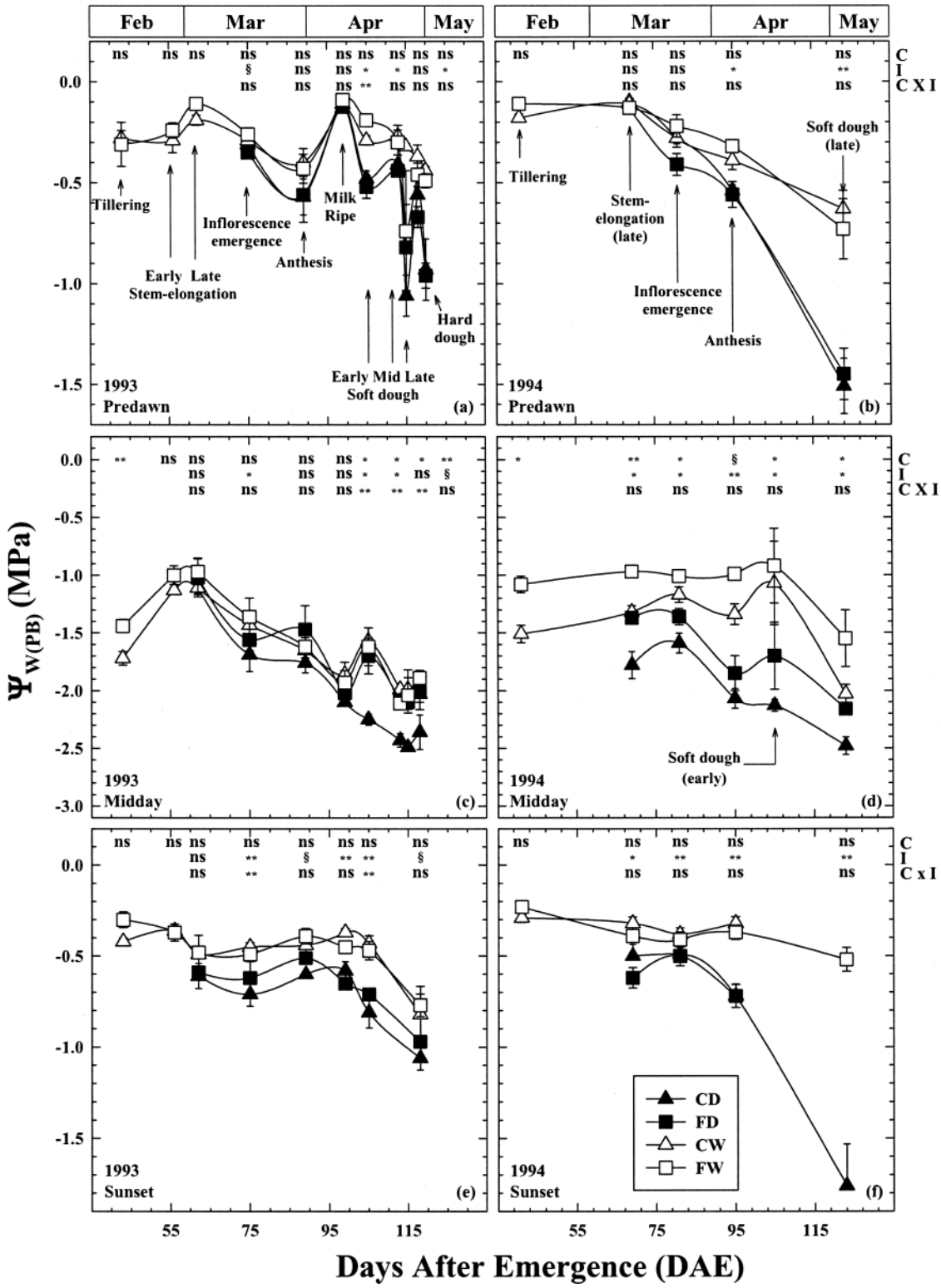

Fig. 4. Dawn to dusk trends in mean total leaf water potential measured with a pressure chamber ($\Psi_{W(PB)}$) in fully expanded sunlit spring wheat leaves at (a, b) predawn, (c, d) midday (solar noon), and (e, f) sunset for day after 50% emergence (DAE) 43 to 118 during the (a, c, e) 1993 and DAE 41 to123 during the (b, d, f) 1994 growing seasons. Measurement dates correspond with up-pointing arrows shown in Fig. 1b, d. Each mean datum is the pooled average of three to four leaves collected within a 15-min period in four replicate blocks (i.e., means based on $n = 12$ or $n = 16$). Vertical bars are 1 SE of replication means (i.e., $n = 4$). Symbols in legend, source of variance, and results from ANOVA are the same as described in Fig. 1. Note that the *y* axis scale for (a, b) predawn and (e, f) sunset are the same, but the scale for (c, d) midday is double that of predawn and sunset. The above illustration was derived from measurements of as many as 2304 leaves.

a proportionate midafternoon depression in g_s by as much as 25% (Fig. 2). Therefore, we accept Hypothesis 2.

Plant Water Relations

Hypothesis 3: During the diurnal period, when transpiration rates are at their maximum, elevated C_a will improve (less negative) midday Ψ_W, and during the nocturnal period greater recovery in plant water status will be observed at predawn and sunset

More negative Ψ_M usually cause more negative Ψ_W and Ψ_π, and lower Ψ_P in field-grown wheat in both irrigated and dryland soil moisture regimes (Denmead and Millar, 1976; Millar and Denmead, 1976). Our results were consistent with this trend because as θ_S became depleted throughout the ontogeny of the crop, Ψ_M became more negative (Fig. 1a, c). And as Ψ_M became more negative, season-long values of $\Psi_{W(PB)}$ also became progressively more negative (Fig. 3 and 4). Furthermore, $\Psi_{W(PB)}$ was significantly more negative in Dry than Wet and for Control compared with FACE (Fig. 3; Tables 1, 3), thereby resulting in a treatment response ranking (i.e., less negative) for $\Psi_{W(PB)}$ of FW > CW > FD > CD (Fig. 3). During 1993, the first significant $C \times I$ interaction effect for $\Psi_{W(PB)}$ was observed at MA during inflorescence emergence on DAE 75 (Fig. 3a), but during 1994 it occurred one soil dehydration cycle earlier at stem-elongation on DAE 69 (Fig. 3g). These significant $C \times I$ interaction effects occurred because, on a relative basis, a greater disparity in $\Psi_{W(PB)}$ was observed between FD and CD than between FW and CW.

At predawn and sunset, the dependency of $\Psi_{W(PB)}$ on Ψ_M was more pronounced in Dry than Wet (Tables 1, 3). Although FACE fostered greater recovery in values of $\Psi_{W(PB)}$ to almost predawn (Fig. 4a, b) levels by sunset (Fig. 4e, f), over the nocturnal period, enough time had elapsed to enable recovery of predawn value of $\Psi_{W(PB)}$ to that of Ψ_M, regardless of C_a level. Nevertheless, FACE caused slightly less negative values of $\Psi_{W(PB)}$ at both predawn and sunset.

The θ_S became the most depleted during the third and fourth soil dehydration cycles (see circled letters e–j; Fig. 1c). Although water stress was mild during the third soil dehydration cycle (DAE 96, 106) (Fig. 1c), $\Psi_{W(PSY)}$ was less negative and Ψ_π was more negative in FACE compared with Control (Fig. 5b). But, little difference in Ψ_P was observed (Fig. 5a). In contrast, during the fourth soil dehydration cycle, a parabolic trend reversal in Ψ_P occurred as θ_S became depleted from fully rehydrated (Ψ_P: ranking of CD > FD > CW > FW) at mid milk ripe on DAE 111 to dehydrated (Ψ_P: ranking of FW > CW > FD > CD) at soft dough on DAE 124, as evidenced by a significant $C \times I$ interaction during the fourth soil dehydration cycle on DAE 120 (Fig. 5a). Following soil rehydration on DAE 111 (Fig. 1c), greater recovery in Ψ_P occurred between CD and FD than between CW and FW. As the number of days since the last irrigation in the Dry treatments increased from 1 on DAE 111 to 14 on DAE 124 (Fig. 1c), compared with CD, $\Psi_{W(PSY)}$ for FD remained less negative and Ψ_π became more negative (Fig. 5b). This resulted in more positive Ψ_P (Fig. 5a). This parabolic trend reversal in Ψ_P between FACE and Control occurred despite the fact that at soft dough on DAE 124 Ψ_M became as negative as −0.91 MPa in FD but was only −0.27 MPa in Control (Fig. 1c).

Regardless of C level, $\Psi_{W(PSY)}$ and Ψ_π became more negative with increasingly negative Ψ_M. But, as $\Psi_{W(PSY)}$ became increasingly negative, Ψ_π became negative 11% slower for Control than for FACE ($P = 0.20$) (Fig. 5c). When Ψ_M was at its most negative at −0.91 MPa at soft dough on DAE 124 (Fig. 1c), Ψ_π was −3.2 MPa in Control compared with −3.7 MPa in FACE (Fig. 5c). Conversely, as $\Psi_{W(PSY)}$ became increasingly negative, Ψ_P became less positive 11% faster for Control than for FACE ($P = 0.20$) (data not shown). When Ψ_M was at its most negative at −0.91 MPa at soft dough on DAE 124, Ψ_P was 0.33 MPa less in Control (0.50 MPa) than FACE (0.83 MPa).

These results clearly demonstrate that lower g_s in FACE compared with Control (Fig. 2) lowered TR (Table 3) in both Wet and Dry, thereby reducing internal plant water deficits, which resulted in less negative $\Psi_{W(PB)}$, particularly during MD and MA (Fig. 3–5). Ultimately, improved water relations during the diurnal period occurred because elevated C_a reduced water stress–induced midafternoon depression in A (Fig. 6, 7a, b), thereby enabling an increase in carbon gain for both A' (Fig. 11) and A'' (Fig. 12). A similar elevated C_a–based improvement in water relations occurred during the nocturnal period because less recovery in $\Psi_{W(PB)}$ in response to more negative Ψ_M was required at predawn (Fig. 4a, b) and sunset (Fig. 4e, f). Hence, we accept Hypothesis 3.

Hypothesis 4: Under more severe drought conditions, elevated C_a will enhance $\Delta\Psi_\pi$, thereby resulting in a decrease in $\Delta\Psi_P$, as evidenced by leaves that maintain higher values of Ψ_P

Sionit et al. (1980a, 1980b, 1981a, 1981b) demonstrated that as initially irrigated plants experienced a drought cycle the stomata of leaves grown at ambient C_a closed faster at less negative Ψ_W than those grown in elevated C_a. Results reported herein support this interpretation because, as Ψ_M became more negative with depletion of θ_S (Fig. 1a, c), g_s was greater for elevated C_a plants. The higher g_s occurred because stomata of plants grown in elevated C_a did not close until Ψ_M was −1.1 MPa, whereas those of plants grown in ambient C_a closed at a Ψ_M of −0.24 MPa (Wall, 2001). For a given Ψ_W, elevated C_a caused more negative Ψ_π that improved the ability of wheat leaves to maintain greater Ψ_P, and thus higher g_s. Maintaining higher g_s for a longer period into a drought cycle resulted in greater overall carbon gain. In a companion study of wheat ears, Wechsung et al. (2000) reported that elevated C_a caused an even greater reduction in g_s of ears to water deficits than that reported herein for leaves. Since ears accumulate even more TNC than leaves for osmotic adjustment (Morgan, 1980a, 1980b), the reduction in g_s of ears in response to water deficits may have also resulted from an elevated C_a–induced enhancement in accumulation of osmotic solutes.

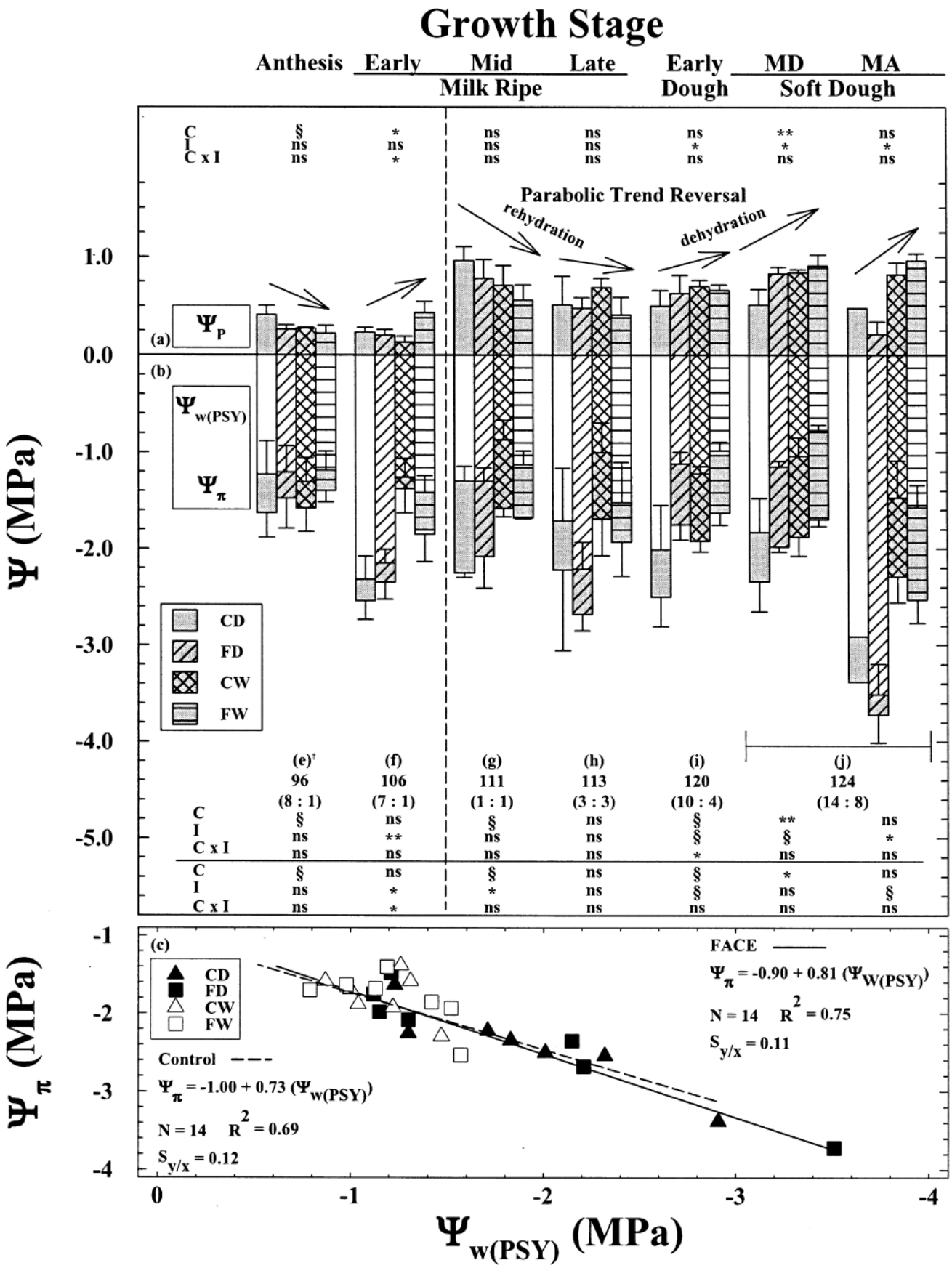

Under more severe water stress, leaves lose turgor pressure because, as Ψ_W becomes more negative (with more negative Ψ_M), Ψ_π becomes more negative at a slower rate, which results in less positive Ψ_P in wheat leaves (Johnson et al., 1984; Morgan and Condon, 1986; Kameli and Losel, 1994). However, osmoregulatory mechanisms of plants enable them to maintain more positive Ψ_P for a longer period into a drought (Kirkham, 1990). In our study, elevated C_a affected the relative change in Ψ_W with respect to Ψ_π because, as Ψ_M became more negative, $\Delta\Psi_\pi$ was 11% greater resulting in an 11% decrease in $\Delta\Psi_P$ (Fig. 5c). This C_a–based enhancement in osmoregulation was most evident in the fourth soil dehydration cycle during 1994 because, over a 14-d interval (DAE 111–DAE 124; see circled letters g–j in Fig. 1c), following an irrigation on DAE 110 that rehydrated the soil profile, a parabolic trend reversal in Ψ_P occurred (Fig. 5a). Since elevated C_a is known to alleviate drought stress (Wall, 2001; Wall et al., 2001a; Wullschleger et al., 2002), leaves grown under elevated C_a require less recovery following soil rehydration. In contrast, leaves grown under current ambient C_a levels were the most stressed and required much greater recovery. As many as three soil dehydration cycles had already occurred for the Dry treatments (Fig. 1c), so that wheat plants had already become acclimated to drought. Apparently, elevated C_a enhanced this acclimation response because an increase in osmotic adjustment decreased the plasticity in response of wheat leaves to environmental constraints such as drought. This was also observed in spring wheat grown in controlled-environment growth cabinets maintained at 350 and 1000 μmol mol^{-1} CO_2 by Sionit et al. (1981a, 1981b), who reported that elevated C_a consistently caused less negative Ψ_W, more negative Ψ_π, and more positive Ψ_P. They reported that at the end of the second soil dehydration cycle during grain filling, after leaves had become preconditioned to drought, Ψ_π was −1.8 MPa compared with −2.1 MPa for 350 and 1000 μmol (CO_2) mol^{-1}, respectively. Results reported herein were similar because on the last sampling date on DAE 124 1994 when Ψ_M was as negative as −0.91 MPa (Fig. 1c), Ψ_π was −3.2 MPa compared with −3.7 MPa for ambient and elevated C_a, respectively (Fig. 5). Interpolating results from Sionit et al. (1981a, 1981b) during their second dehydration cycle (between anthesis and grain filling), $\Delta\Psi_\pi$ was 0.50 at ambient C_a (350 μmol mol^{-1}) and 0.75 at elevated C_a (1000 μmol mol^{-1}). A 650 μmol mol^{-1} increase in C_a, therefore, induced a 50% increase in $\Delta\Psi_\pi$, whereas herein we report that a 180 μmol mol^{-1} increase in C_a induced an 11% increase in $\Delta\Psi_\pi$ (Fig. 5). Between these two wheat experiments, a 4.5-fold difference in $\Delta\Psi_\pi$ may have occurred, in part, because of the 3.6-fold difference between C_a treatment levels. Allen et al. (1998) also reported that, as θ_S was depleted over a 4-d period during pod-fill for soybean grown in controlled-environment sunlit cabinets maintained at 330 and 660 μmol (CO_2) mol^{-1}, elevated C_a also enabled water-stressed soybean leaves to maintain higher levels of Ψ_P.

Presumably, an increase in A because of elevated C_a (Fig. 6) resulted in higher leaf TNC content (Fig. 8 and 9), as reported elsewhere (Hendrix, 1992; Hendrix et al., 1994; Drake et al., 1997). In elongating and fully expanded zones of leaves of water-stressed wheat seedlings grown at ambient C_a and high light intensities (i.e., high availability of organic solutes), an increase in osmotic adjustment was positively correlated with higher TNC pools (Munns et al., 1979; Munns and Weir, 1981). Blum et al. (1988) showed a positive correlation between the accumulation of TNC and stomatal aperture in wheat, presumably because osmoregulation enables wheat leaves to tolerate drought. Hence, an increase in the TNC pool because of an elevated C_a–based stimulation of A (Fig. 3) may have contributed to an increase in the accumulation of osmotica in vacuoles (Acevedo et al., 1979; Pollock, 1986; Chatterton et al., 1987), thereby explaining an increase in $\Delta\Psi_\pi$ (Fig. 5c). Therefore, we accept Hypothesis 4.

Stomatal and Nonstomatal Limitations to Carbon Gain

Hypothesis 5: Under ample water supply any reduction in carbon gain will occur mostly because of nonstomatal limitations, whereas under drought conditions stomatal limitations will reduce carbon gain

The treatment response ranking for A was FW > FD ≅ CW > CD (Fig. 6)—nearly the inverse of that for g_s (Fig. 2). Compared with Wet, Dry significantly reduced A, whereas compared with Control, FACE significantly increased A (Fig. 6; Tables 1, 3). Significant $C \times I$ interaction effects occurred because elevated C_a reduced water stress–induced depressions in carbon-gain, particularly at MD (Fig. 6; Tables 1, 3). This resulted in a hysteresis effect when A vs. PPFD was plotted from dawn until MD compared with that from

Fig. 5. Mean (b) total leaf water ($\Psi_{W(PSY)}$), and (b) osmotic (Ψ_π) potentials determined using standard thermocouple psychometric techniques, and the (a) resultant pressure (Ψ_P) potential (i.e., $\Psi_P = \Psi_{W(PSY)} - \Psi_\pi$) for fully expanded sunlit flag leaves of spring wheat at midday (MD) (solar noon) and at midafternoon (MA) (2.5 h after solar noon) on day after 50% emergence (DAE) and development stage given during the 1994 growing season. † Letters e through j in legend of panel (b) denote DAE and number of days between measurement dates and last irrigated for (Dry:Wet) treatments during the third (e, f) and fourth (g, h, i, and j) soil dehydration cycles (Fig. 1c). Vertical dashed lines in panels (a) and (b) delineate the third and fourth soil dehydration cycles illustrated in Fig. 1c. Horizontal arrows in panel (a) denote overall trend in values of Ψ_P across treatments. Each mean datum for $\Psi_{W(PSY)}$, Ψ_π, and the resultant Ψ_P was derived from three repeated measures across four treatments and three replications ($3 \times 4 \times 3$) when Model C-30s psychrometers were used at MD on DAE 120 and MA on DAE 124, and four repeated measurements across four treatments and three replications ($4 \times 4 \times 3$) when Model 84-3vC J.D.J. Merrill Specialty Equipment, Longan, UT, were used at MD (DAE 96, 106, 111, 113, 124) (i.e., means based on $n = 36$ or $n = 48$, respectively). Vertical bars are 1 SE of replication means (i.e., $n = 3$). Symbols in legend, source of variance, and results from ANOVA same as described in Fig. 1. Regression of Ψ_π on $\Psi_{W(PSY)}$ (i.e., rate of change in osmotic potential; $\Delta\Psi_\pi$) from anthesis until soft dough for fully expanded sunlit flag leaves of (c) spring wheat. Summary statistics for a linear regression are as follows: N, number of observations; R^2, coefficient of determination; $S_{y/x}$, SE of y given a value of x. The above illustration was derived from measurements from as many as 312 leaves.

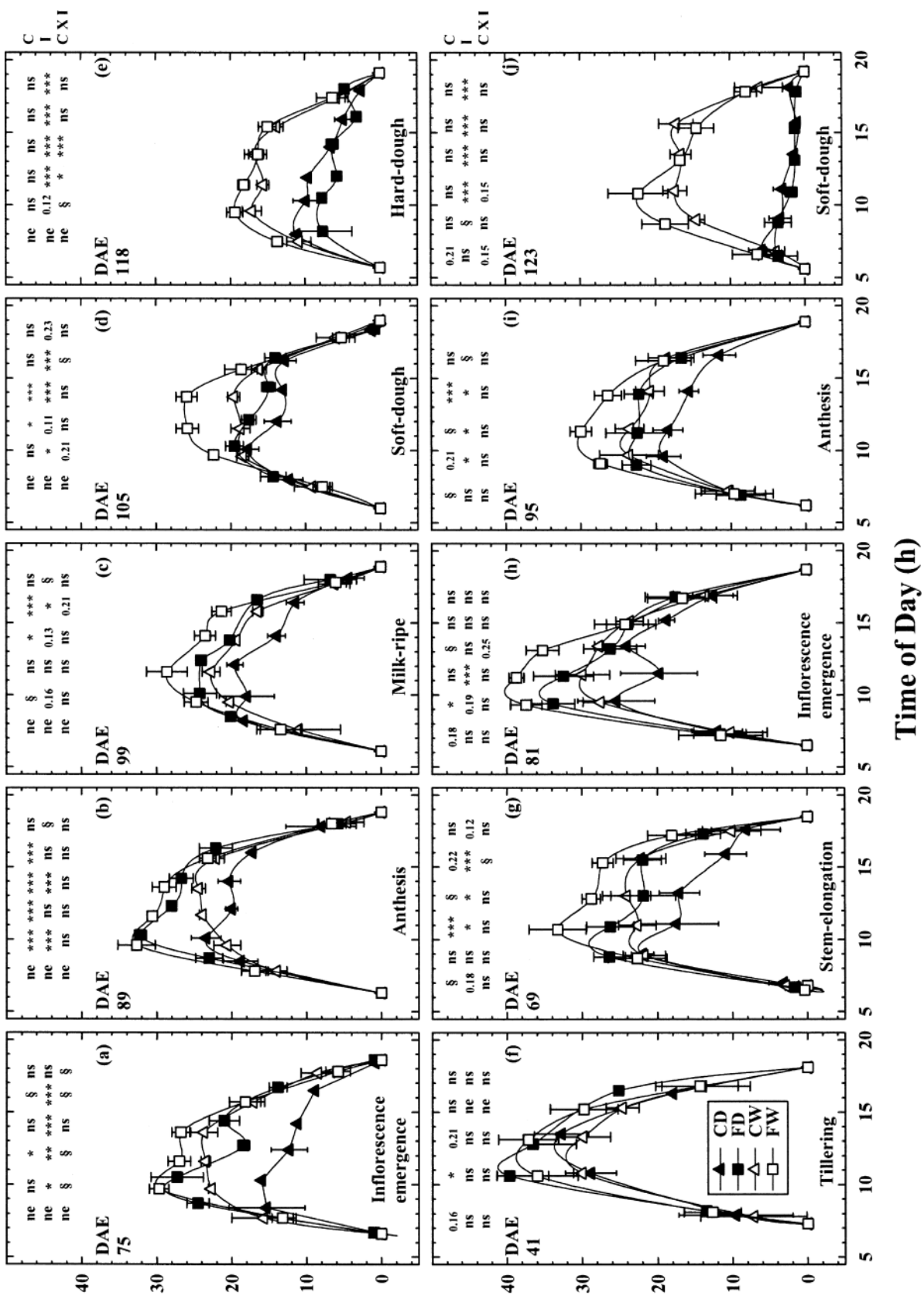

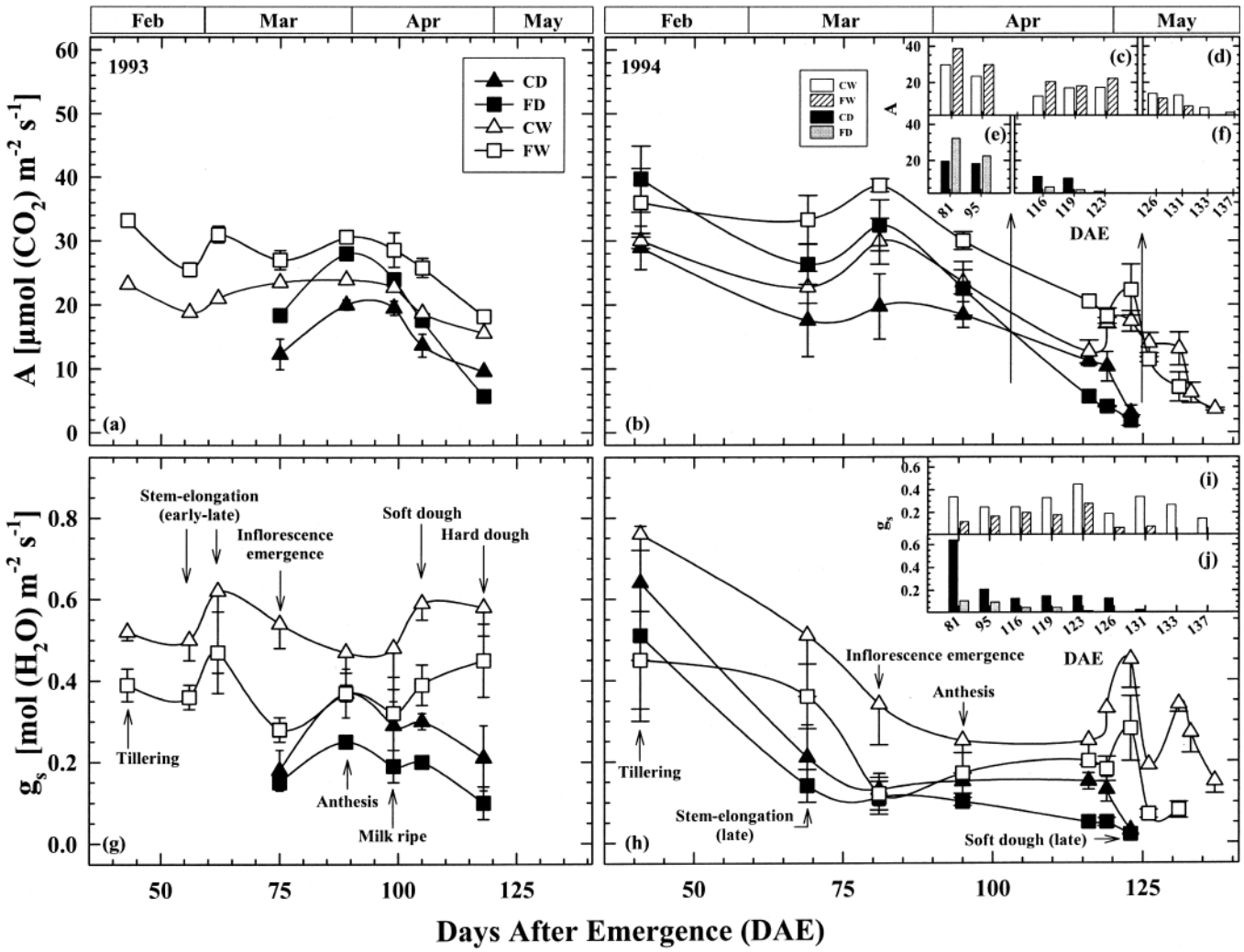

Fig. 7. Mean maximum midday (MD: solar noon) net assimilation rate (*A*) (a, b) and stomatal conductance to water vapor (g_s) (g, h) for fully expanded sunlit spring wheat leaves for day after 50% emergence (DAE) and development stages given during the (a, g) 1993 and (b, h) 1994 growing seasons, respectively. Histograms shown during 1994 in panel b (inserts c, d, e, and f) illustrate values of *A* from inflorescence emergence (DAE 81) until physiological maturity for (c, d) Wet (DAE 137) and (e, f) Dry (DAE 123) treatments, a period of accelerated senescence. Treatment inversion in the carbon dioxide (*C*) effect on values of *A* are denoted by up-pointing arrows in panel (b), which intersect approximately on DAE 124 (histogram panels c and d) for Wet, and on DAE 103 (histogram panels e and f) for Dry treatments. Histograms shown during 1994 in panel (h) (inserts i and j) illustrate values of g_s for (i) Wet and (j) Dry treatments. Unlike the treatment inversion observed in the *C* effect for *A* (inserts c, d, e, f), no such effect was observed in g_s (i, j). All measurements were simultaneous with, and sampled as described for g_s in Fig. 2 and for *A* in Fig. 6. Symbols in legend, source of variance, and results from ANOVA same as described in Fig. 1. The above illustration was derived from measurements of as many as 960 leaves.

MD to dusk (Fig. 10a). Across years and development stages, this hysteresis effect appeared to be greater at inflorescence emergence on DAE 81 (Fig. 6h). Although a minor hysteresis effect occurred for CW on DAE 81, it was more pronounced in CD (Fig. 10a). In contrast, under elevated C_a, hysteresis patterns were more similar between Wet and Dry plots. The hysteresis effect on *A* became more pronounced as θ_S became more depleted later in the ontogeny of the crop. Relationships between *A* and PPFD from dawn to MD and from MD to dusk were normalized (A_n) by dividing each observation of *A* within a day by the maximum value of *A* (A_{max}) for that day (Fig. 10b). All values of A_n were pooled across years and development stages, except during senescence at hard-dough (DAE 118) during 1993 and soft dough (DAE 123) during 1994. Clearly, no hysteresis effect occurred under CW, a slight hysteresis effect was observed under FW, but only a modest increase in this effect was observed for FD. In contrast, a large hysteresis effect was observed for CD. These hysteresis effects occurred primarily because of a midafternoon depression in leaf *A* (Fig. 6). The degree of hysteresis

Fig. 6. Dawn to dusk trends in mean leaf net assimilation rate (*A*) of fully expanded sunlit spring wheat leaves for day after 50% emergence (DAE) and development stages given for 5 d during the (a–e) 1993 and (f–j) 1994 growing seasons. Measurements were simultaneous with and sampled as described for g_s in Fig. 2. Symbols in legend, source of variance, and results from ANOVA same as described in Fig. 1. The above illustration was derived from measurements of as many as 3540 leaves.

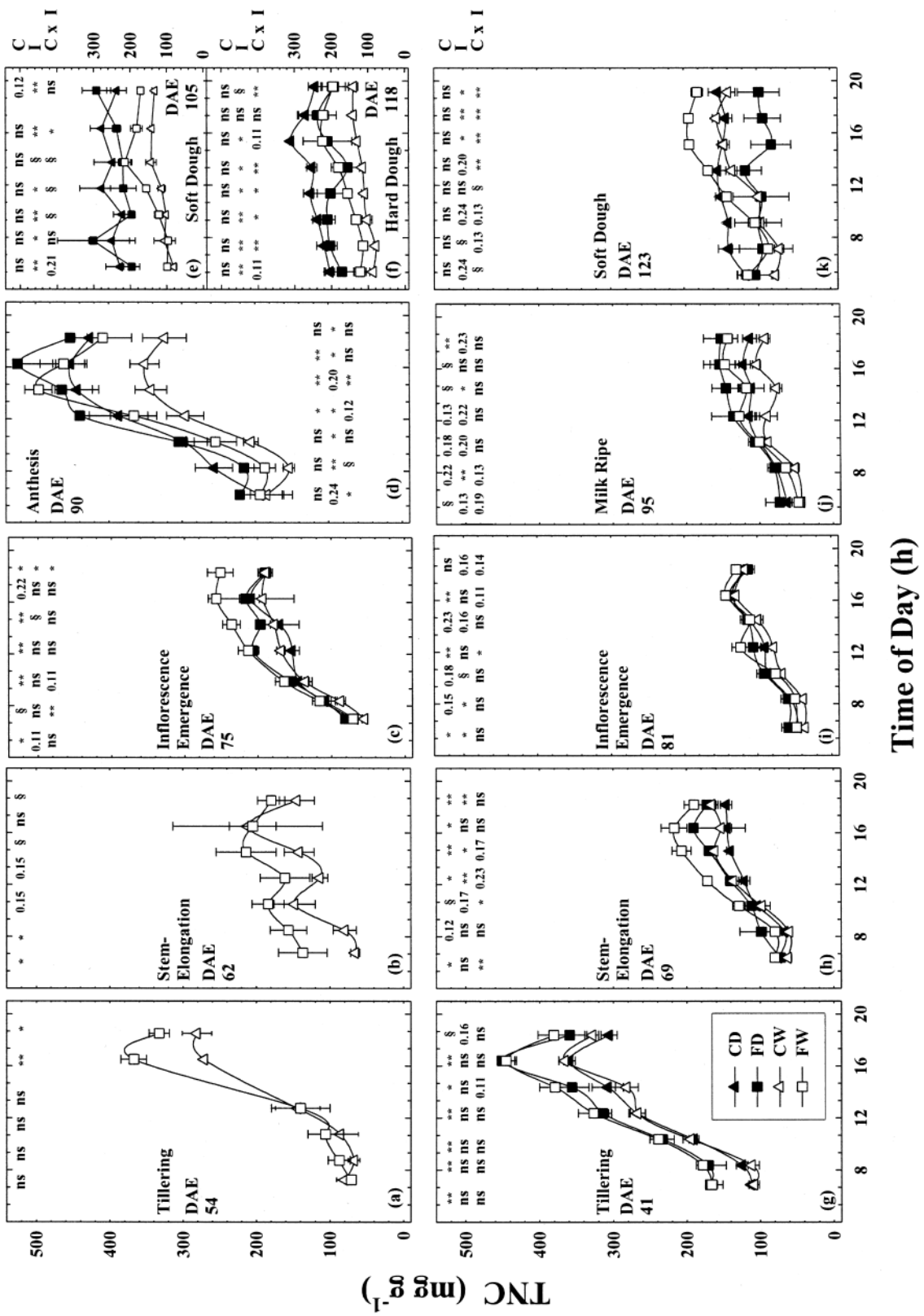

Fig. 8. Dawn to dusk trends in mean leaf total nonstructural carbohydrates (TNC), consisting of water-soluble sugars (glucose, fructose, sucrose), low and high molecular weight fructans, and starch. Uppermost fully expanded sunlit spring wheat leaves were sampled for day after 50% emergence (DAE) and development stages given for 6 d during the 1993 (a–f) and 5 d during the 1994 growing seasons (g–k) (note that during 1993 panels (e) and (f) are denoted by the right-most *y* axis, which is scaled half that of the left-most *y* axis). Symbols in legend, source of variance, and results from ANOVA are the same as described in Fig. 1. Each mean datum was derived from four individual assays (repeated measures) performed on a 30-mg sample (i.e., pooled sample taken from the thoroughly mixed powder of 10 freeze-dried leaves) across four replications at 2-h sample intervals (i.e., means based on $n = 16$). Vertical bars are 1 SE of replication means (i.e., $n = 4$). The above illustration was derived from measurements of as many as 9120 leaves.

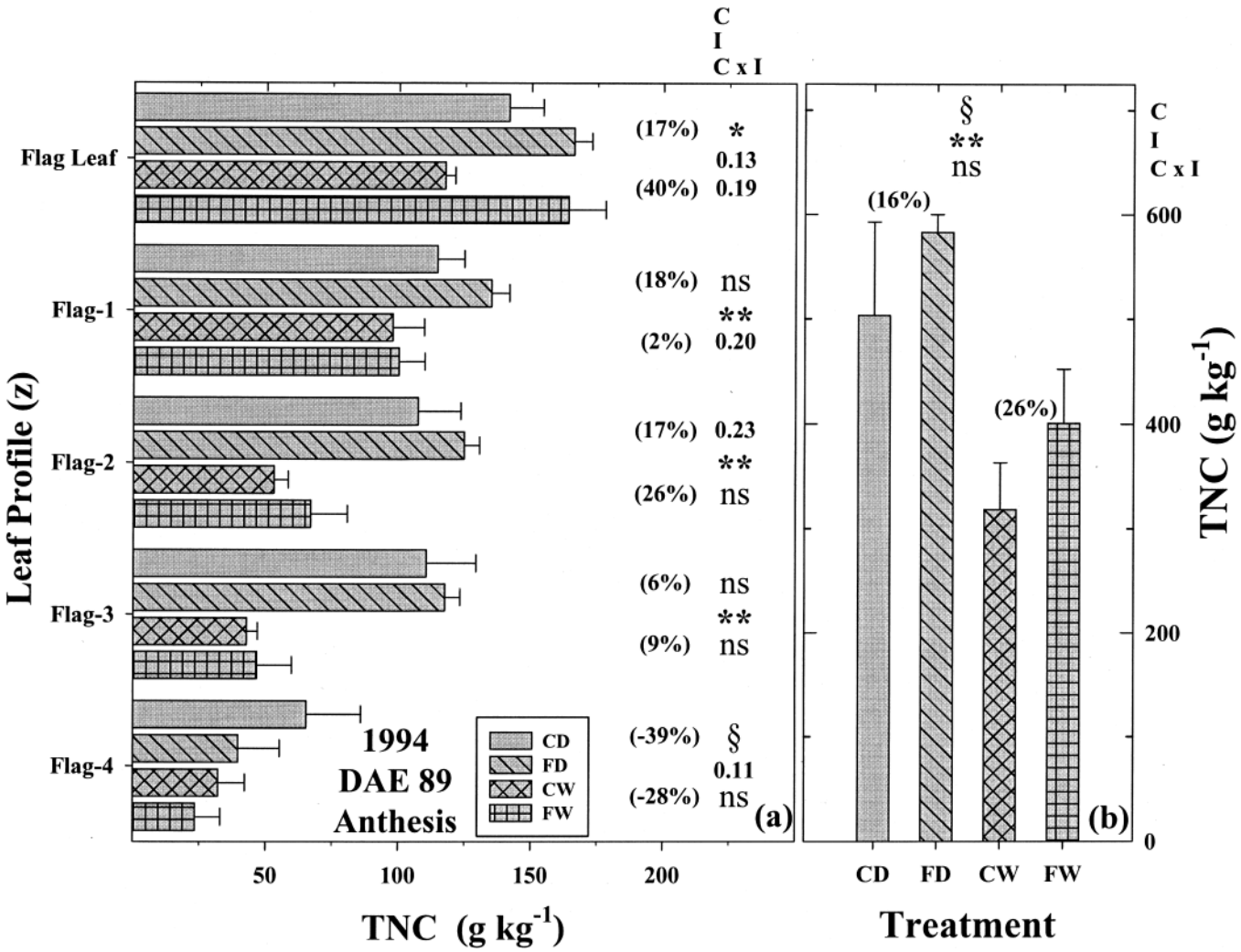

Fig. 9. Midday (MD: solar noon) trends in leaf tissue total nonstructural carbohydrate concentration (TNC) (i.e., water-soluble sugars (glucose, fructose, sucrose), low and high molecular weight fructans, and starch). (a) At anthesis (day after emergence, DAE) 89 during 1994, the uppermost fully expanded sunlit flag leaf and all physiologically active leaves beneath the flag leaf (i.e., flag-1, flag-2, flag-3, and flag-4) were sampled in sequential order from the same culm, for each of 10 culms, from the top of the canopy height (*Z*) denoted by the left-most *y* axis. (b) The whole-canopy TNC profile represents the sum of the flag through flag-4 leaves denoted by right-most *y* axis. Each mean datum was derived from four individual assays (repeated measures) performed on a 30-mg sample (i.e., pooled sample taken from the thoroughly mixed powder of 10 freeze-dried leaves) across four replications sampled at MD (i.e., means based on $n = 16$). Symbols in legend and results from ANOVA same as described in Fig. 1. Vertical bars are 1 SE of replication means (i.e., $n = 4$). Percentages in parentheses above each mean histogram datum indicate relative CO_2 enhancement at Dry and Wet, respectively. Source of variance in ANOVA are as follows: replication (*R*); CO_2 (*C*); irrigation (*I*); and, canopy height (*Z*). The corresponding error term for each effect is given in parenthesis as follows: *C* ($R \times C$); *I* ($R \times I$); $C \times I$ ($R \times C \times I$); *Z* ($R \times Z$); $Z \times C$ ($R \times Z \times C$); $Z \times I$ ($R \times Z \times I$); $Z \times C \times I$ ($R \times Z \times C \times I$). The above illustration was derived from measurements of as many as 800 leaves.

was proportional to any stomatal and/or nonstomatal limitations to carbon gain, whereas the amount of potential carbon loss was directly proportional to the integrated area within the hysteresis loop (Fig. 10).

The minor hysteresis effect observed in leaves grown in elevated C_a and adequate water supply is more likely because of nonstomatal (i.e., biochemical-based transient inhibition in photosynthetic capacity) (Farquhar and Sharkey, 1982; von Caemmerer and Farquhar, 1984; Krapp et al., 1991, 1993; Stitt, 1991) rather than stomatal limitation. Furthermore, production of assimilates in excess of phloem loading capacity can result in an accumulation of TNC in source leaves that can cause physical damage, thereby disrupting electron transport at the chloroplast level (Neales and Incoll, 1969; Azcón-Bieto, 1983; Foyer, 1988). Nevertheless, in a companion study, Nie et al. (1995a, 1995b) found no indication of any damage to chloroplast reactions in wheat leaves exposed to FACE until senescence. This is in agreement with the belief of Sharkey and Seemann (1989), who reported that any reduction in carbon gain resulting from mild water stress occurred because of stomatal rather than nonstomatal limitation.

At midday during inflorescence emergence (DAE 75), a period of rapid growth when sink limitations usually does not limit carbon uptake, leaf starch levels were 67% greater at elevated (10 g kg^{-1}) compared with ambient (6 g kg^{-1}) C_a, and by dusk they more than doubled,

Table 2. Means ± standard error (SE) across both years and all soil dehydration cycles for field-grown spring wheat [*Triticum aestivum* (L.) cv. Yecora Rojo] reared under two atmospheric carbon dioxide concentrations [Control (*C*) at 370 μmol mol^{-1}, FACE (F) at ambient +180 μmol mol^{-1}], and two irrigation regimes [Dry (*D*) at 50%, Wet (*W*) at 100% replacement of evapotranspiration] during the 1993 and 1994 growing seasons. Season-long average given for edaphic parameters include volumetric soil–water content (θ_S), soil matric potential (Ψ_M), evapotranspiration rate (ET), and cumulative evapotranspiration (ET_c) obtained from Hunsaker et al. (1996). Growth parameters include season-long average living root (B_R) and total shoot (B_S) biomass, root to shoot ratio (B_R/B_S), and the season-long maximum living root ($B_{R(max)}$) and total shoot ($B_{S(max)}$) biomass. Also shown are the ratios of the carbon dioxide (*F*/*C*) and irrigation (*D*/*W*) treatments.

Parameter	Irrigation	Control	FACE	*F*/*C*
		Edaphic†—season-long averages		
θ_S, m^3 m^{-3}	*D*	0.23 ± 0.01	0.22 ± 0.01	0.96
	W	0.27 ± 0.01	0.28 ± 0.01	1.04
	D/*W*	0.85	0.79	
Ψ_M, MPa	*D*	−0.24 ± 0.08	−0.53 ± 0.08	2.21
	W	−0.03 ± 0.01	−0.10 ± 0.03	3.33
	D/*W*	8.00	5.30	
ET, mm d^{-1}	*D*	4.2 ± 0.1	4.3 ± 0.2	1.30
	W	5.9 ± 0.2	5.7 ± 0.1	0.96
	D/*W*	0.70	0.76	
ET_c, mm	*D*	446 ± 11	459 ± 18	1.03
	W	642 ± 18	610 ± 13	0.95
	D/*W*	0.70	0.75	
		Growth‡—season-long averages		
B_S, g m^{-2}	*D*	51 ± 2	58 ± 4	1.15
	W	58 ± 2	67 ± 4	1.15
	D/*W*	0.87	0.87	
B_R, g m^{-2}	*D*	50 ± 3	62 ± 5	1.25
	W	49 ± 3	62 ± 6	1.26
	D/*W*	1.01	1.00	
B_R/B_S	*D*	0.36 ± 0.19	0.40 ± 0.29	
	W	0.38 ± 0.25	0.39 ± 0.43	
	D/*W*			
		Growth‡—season-long maximum		
$B_{S(max)}$, g m^{-2}	*D*	1439 ± 46	1568 ± 37	1.09
	W	1844 ± 24	1957 ± 41	1.06
	D/*W*	0.78	0.80	
$B_{R(max)}$, g m^{-2}	*D*	93 ± 7	128 ± 15	1.38
	W	89 ± 11	117 ± 5	1.32
	D/*W*	1.05	1.10	

† Edaphic parameter (i.e., θ_S, Ψ_M, ET, ET_c) treatment means were obtained from four replications (i.e., means based on $n = 4$, SE of replication mean based on $n = 4$).

‡ Growth parameter for shoot (i.e., B_S, $B_{S(max)}$) treatment means based on four replications (i.e., means based on $n = 4$, SE of replication mean based on $n = 4$). Growth parameter for living root (i.e., B_R, $B_{R(max)}$) and root to shoot ratio (i.e., B_R/B_S) derived from four replications during vegetative development (i.e., 3-leaf, tillering, stem-elongation) and two replications during reproductive development (i.e., anthesis, grain filling, final harvest) (i.e., means and SE of replication means based on $n = 4$ and $n = 2$, respectively).

reaching 27 g kg^{-1} in elevated compared with 12 g kg^{-1} in ambient C_a (Nie et al., 1995a). Furthermore, by dusk the TNC content reached 250 g kg^{-1} in elevated compared with 195 g kg^{-1} in ambient C_a (Fig. 8c). And at anthesis (DAE 90, 1993), when sink demand for the developing kernels during reproductive development was even greater than that at inflorescence emergence during vegetative development, elevated C_a more than doubled these aforementioned effects (Fig. 8d). Further evidence for this phenomenon was observed by comparing the TNC content in the flag leaf of the whole-canopy profile during 1994 (Fig. 9a) with midday values of TNC during anthesis in 1993 (Fig. 8d). Clearly, throughout the diurnal period export of carbon from the leaves lagged behind production. A similar elevated C_a–based increase in TNC pools occurred for all development stages except during the onset of senescence at late grain filling (Fig. 8f, k). Only a minor hysteresis effect was observed for well-watered ambient C_a Control leaves (Fig. 10a) (presumably, export of carbon from the leaves kept pace with synthesis), whereas a much greater hysteresis effect was observed for well-watered elevated C_a leaves (presumably, export of carbon from the leaves lagged behind synthesis). Therefore, the observed hysteresis effect for well-watered leaves grown under elevated C_a (Fig. 10b) can be explained by accumulation of carbon that probably caused nonstomatal limitation such as photoinhibition (Azcón-Bieto, 1983; DeLucia et al., 1985).

Compared with the substantial reduction in g_s due to FACE under well-watered conditions, FACE caused only a nominal decrease in g_s of the water-stressed plants (Table 2, Fig. 2), and only a slightly greater hysteresis loop than that of well-watered wheat was observed (Fig. 10b). Consequently, we believe that the bulk of the potential loss in daily carbon gain within the hysteresis loop (Fig. 10b) resulted from nonstomatal rather than stomatal factors, and we accept Hypothesis 5.

Hypothesis 6: On a relative basis, the net gain in carbon uptake in response to elevated C_a will be proportionately greater under dry than wet

Essentially no hysteresis occurred in well-watered, ambient C_a grown leaves (Fig. 10b) where g_s was nonlimiting, and TNC pools were much lower than in elevated C_a leaves (Fig. 9). However, a large hysteresis effect was observed for leaves grown under water stress and ambient C_a (Fig. 10b). Undoubtably, stomatal factors were responsible for the hysteresis effect observed in water-stressed, ambient C_a leaves because mild water stress should not damage chloroplast reactions (Sharkey and Seemann, 1989). Furthermore, water stress–induced reductions in g_s were observed (Fig. 2 and 7g, h), and TNC pools were much lower in ambient than in elevated C_a leaves (Fig. 8). Apparently, these stomatal limitations were severe enough to limit substrate availability at the site of carboxylation, thereby resulting in midafternoon depressions in carbon gain for water-stressed, ambient C_a leaves (Boyer, 1971; Sionit et al., 1981a, 1981b; Tenhunen et al., 1980; Tenhunen, 1984). Under water stress conditions, therefore, elevated C_a minimized stomatal limitation, which enabled greater carbon gain for a longer period into the drought. These results also demonstrate, however, that although leaves grown under elevated C_a will have less stomatal limitation, regardless of water supply, they will still experience some midafternoon depression in *A* because of nonstomatal limitation. Therefore, we accept Hypothesis 6.

Table 3. Means ± standard error (SE) across both years and all soil dehydration cycles for field-grown spring wheat [*Triticum aestivum* (L.) cv. Yecora Rojo] reared under two carbon dioxide [Control (*C*) at 370 μmol mol^{-1}, FACE (*F*) at ambient + 180 μmol mol^{-1}], and two irrigation regimes [Dry (*D*) at 50%, Wet (*W*) at 100% replacement of evapotranspiration] during the 1993 and 1994 growing seasons. Gas exchange parameters for fully expanded upper canopy sunlit leaves measured at midmorning (MM: 2 h before solar noon), midday (MD: solar noon) and midafternoon (MA: 2 h after solar noon) include stomatal conductance to water vapor (g_s), net assimilation rate (A), transpiration rate (TR), leaf temperature (T_l), leaf minus air temperature (ΔT), both actual (WUE, A/TR) and intrinsic (IWUE, A/g_s) water use efficiencies, internal CO_2 concentration in mesophyll tissue (C_i) and the ratio of C_i to atmospheric CO_2 concentration (C_a) (C_i/C_a). Water relation parameters include total plant water potential measured with a pressure chamber (bomb) ($\Psi_{W(PB)}$), and total ($\Psi_{W(PSY)}$) and osmotic (Ψ_π) potentials measured with thermocouple psychrometers to derive turgor potential (i.e., $\Psi_P = \Psi_{W(PSY)} - \Psi_\pi$). Carbohydrate parameters include leaf tissue concentrations of simple sugars (CHO: glucose, fructose, sucrose), complex carbohydrates (FRU: low and high molecular weight fructans; *S*: starch), and the total nonstructural carbohydrate (TNC). Also shown are the ratios of the carbon dioxide (F/C) and irrigation (D/W) treatments.

		Control	FACE	F/C	Control	FACE	F/C	Control	FACE	F/C
Parameter	**Irrigation**	**Midmorning**			**Midday**			**Midafternoon**		
					Gas exchange†					
g_s, mol H_2O m^{-2}s^{-1}	*D*	0.28 ± 0.04	0.18 ± 0.02	0.64	0.23 ± 0.03	0.16 ± 0.02	0.70	0.20 ± 0.03	0.16 ± 0.01	0.80
	W	0.48 ± 0.03	0.32 ± 0.02	0.67	0.56 ± 0.07	0.37 ± 0.05	0.66	0.56 ± 0.02	0.32 ± 0.03	0.57
	D/W	0.58	0.56		0.41	0.43		0.36	0.50	
A, μmol CO_2 m^{-2}s^{-1}	*D*	17.3 ± 1.1	23.7 ± 1.4	1.37	17.0 ± 0.8	21.1 ± 1.2	1.24	12.4 ± 0.6	17.8 ± 0.6	1.44
	W	21.4 ± 0.8	28.2 ± 0.8	1.32	21.9 ± 0.4	27.8 ± 0.4	1.27	20.9 ± 0.7	24.5 ± 0.9	1.17
	D/W	0.81	0.84		0.77	0.76		0.59	0.73	
TR, mmol H_2O m^{-2}s^{-1}	*D*	5.9 ± 1.3	4.8 ± 0.9	0.82	7.0 ± 1.6	5.7 ± 1.0	0.81	6.9 ± 1.0	6.3 ± 0.7	0.92
	W	8.0 ± 0.8	6.2 ± 0.6	0.77	11.3 ± 1.5	9.2 ± 1.1	0.82	12.1 ± 0.5	9.0 ± 0.6	0.74
	D/W	0.74	0.78		0.62	0.62		0.57	0.70	
T_l‡, °C	*D*	29.4 ± 0.3	31.0 ± 0.6	1.06	32.0 ± 0.8	33.4 ± 0.8	1.04	33.2 ± 0.6	34.0 ± 0.5	1.02
	W	25.5 ± 0.6	26.6 ± 0.2	1.04	28.6 ± 0.3	30.1 ± 0.3	1.05	29.0 ± 0.3	30.8 ± 0.1	1.06
	D/W	1.15	1.16		1.12	1.11		1.14	1.10	
ΔT‡, °C	*D*	0.08 ± 0.25	0.71 ± 0.13		0.09 ± 0.18	0.50 ± 0.11		−0.03 ± 0.16	0.08 ± 0.06	
	W	−0.35 ± 0.29	−0.05 ± 0.22		−0.89 ± 0.23	−0.39 ± 0.18		−1.03 ± 0.26	−0.55 ± 0.08	
WUE, μmol (CO_2) mmol (H_2O)$^{-1}$	*D*	5.0 ± 1.8	7.0 ± 1.7	1.39	3.2 ± 0.9	4.0 ± 1.6	1.64	2.0 ± 0.2	3.1 ± 0.4	1.56
	W	4.0 ± 0.7	7.4 ± 1.3	1.86	4.0 ± 1.6	5.3 ± 1.6	1.14	2.3 ± 0.2	3.7 ± 0.4	1.58
	D/W	1.26	0.94		0.82	1.77		0.87	0.86	
IWUE, μmol (CO_2) mol (H_2O)$^{-1}$	*D*	98 ± 23	196 ± 45	2.01	86 ± 16	158 ± 31	1.85	68 ± 5	116 ± 15	1.70
	W	62 ± 9	132 ± 25	2.13	67 ± 20	107 ± 14	1.49	48 ± 5	96 ± 7	1.98
	D/W	1.58	1.48		1.28	1.48		1.41	1.21	
C_i, ppm	*D*	191 ± 17	294 ± 26	1.54	196 ± 14	279 ± 32	1.42	210 ± 5	333 ± 13	1.58
	W	222 ± 7	343 ± 20	1.55	227 ± 7	345 ± 16	1.52	234 ± 6	352 ± 10	1.50
	D/W	0.86	0.86		0.86	0.81		0.90	0.95	
C_i/C_a	*D*	0.57 ± 0.06	0.54 ± 0.05	0.95	0.58 ± 0.05	0.51 ± 0.06	0.88	0.62 ± 0.02	0.62 ± 0.03	1.00
	W	0.68 ± 0.03	0.64 ± 0.04	0.94	0.70 ± 0.02	0.65 ± 0.03	0.93	0.72 ± 0.02	0.66 ± 0.02	0.92
	D/W	0.84	0.84		0.83	0.78		0.86	0.94	
					Water relation§					
$\Psi_{W(PB)}$, MPa	*D*	−1.54 ± 0.05	−1.31 ± 0.05	0.85	−1.92 ± 0.03	−1.67 ± 0.03	0.87	−1.84 ± 0.02	−1.61 ± 0.03	0.88
	W	−1.19 ± 0.06	−1.10 ± 0.06	0.92	−1.46 ± 0.03	−1.36 ± 0.05	0.93	−1.46 ± 0.05	−1.24 ± 0.03	0.85
	D/W	1.29	1.19		1.32	1.23		1.26	1.30	
$\Psi_{W(PSY)}$, MPa	*D*				−2.12 ± 0.19	−1.89 ± 0.08	0.89			
	W				−1.18 ± 0.15	−1.16 ± 0.06	0.98			
	D/W				1.80	1.63				
Ψ_π, MPa	*D*				−2.39 ± 0.12	−2.15 ± 0.14	0.90			
	W				−1.77 ± 0.13	−1.70 ± 0.05	0.96			
	D/W				1.35	1.26				
Ψ_P, MPa	*D*				0.53 ± 0.06	0.56 ± 0.04	1.06			
	W				0.67 ± 0.07	0.64 ± 0.03	0.96			
	D/W				0.79	0.88				
					Carbohydrate¶					
CHO, g kg^{-1}	*D*	77 ± 2	74 ± 4	0.96	91 ± 6	89 ± 2	0.98	98 ± 6	94 ± 3	0.96
	W	54 ± 3	65 ± 4	1.19	62 ± 2	78 ± 2	1.24	73 ± 1	100 ± 3	1.38
	D/W	1.42	1.15		1.46	1.15		1.35	0.93	
FRU, g kg^{-1}	*D*	90 ± 4	90 ± 5	1.00	104 ± 5	108 ± 4	1.04	113 ± 6	114 ± 2	1.01
	W	63 ± 3	77 ± 3	1.22	77 ± 2	101 ± 3	1.31	89 ± 2	121 ± 2	1.36
	D/W	1.43	1.17		1.34	1.07		1.28	0.95	
S, g kg^{-1}	*D*	2.7 ± 0.3	3.8 ± 0.3	1.42	4.0 ± 0.3	5.9 ± 0.2	1.48	4.7 ± 0.3	7.6 ± 0.4	1.62
	W	3.1 ± 0.2	4.8 ± 0.3	1.54	4.7 ± 0.2	8.5 ± 0.5	1.80	6.2 ± 0.4	11.1 ± 0.4	1.79
	D/W	0.88	0.81		0.84	0.69		0.76	0.68	

Continued on next page.

Table 3. Continued.

Parameter	Irrigation	Control	FACE	F/C	Control	FACE	F/C	Control	FACE	F/C
		Midmorning			Midday			Midafternoon		
TNC, g kg^{-1}	*D*	169 ± 4	167 ± 8	0.99	198 ± 9	202 ± 6	1.02	216 ± 11	215 ± 4	1.00
	W	120 ± 6	146 ± 6	1.22	144 ± 5	187 ± 5	1.30	168 ± 1	232 ± 5	1.38
	D/*W*	1.41	1.14		1.37	1.08		1.29	0.93	

† Gas exchange parameter (i.e., g_s, A, TR, T_l, ΔT, WUE, IWUE, C_i, C_i/C_a) treatment means were derived from two subsamples (repeated measures) for each of five leaves across two replications for Dry or four replications for Wet during 1993, and three replications for Dry and Wet during 1994 (i.e., during 1993 means based on $n = 20$ for Dry and $n = 40$ for Wet, SE of replication mean based on $n = 2$ for Dry and $n = 4$ for Wet; during 1994 means based on $n = 30$ for Dry and Wet, SE of replication mean based on $n = 3$ for Dry and Wet).

‡ Leaf (T_l) and air (T_a) temperatures measured in 0.25-L cuvette.

§ Water relation parameter treatment means based on pressure chamber (bomb) (i.e., $\Psi_{W(PB)}$) measurements were derived from three to four subsamples (repeated measures) for four replications (i.e., means based on $n = 12$ or $n = 16$, SE of replication mean based on $n = 4$). Water relation parameter treatment means based on thermocouple psychrometers (i.e., $\Psi_{W(PSY)}$, Ψ_π, Ψ_P) were derived from three subsamples (repeated measures) across four treatments and three replications ($3 \times 4 \times 3$) when Model C-30s psychrometers were used and four repeated measurements across four treatments and three replications ($4 \times 4 \times 3$) when Model no. 84-3vC psychrometers were used (i.e., means based on $n = 36$ or $n = 48$, SE of replication mean based on $n = 3$).

¶ Leaf tissue carbohydrate concentration parameter treatment means (i.e., CHO, FRU, *S*, TNC) based on four individual assays (repeated measures) performed for four replications (i.e., means based on $n = 16$, SE of replication mean based on $n = 4$).

Carbon Gain during Senescence

Earlier senescence in Dry compared with Wet reduced g_s and A, but this reduction was most pronounced in FACE compared with Control at MD during 1994 (Fig. 7b). For Dry, the C effect on A inverted on DAE 103 for both years (Fig. 7a, b, e, f), whereas for Wet this treatment inversion occurred 20 d later on DAE 123, 1994 (Fig. 7b, c, d). The absence of positive carbon gain marked the onset of physiological maturity, which occurred 14 d earlier for Dry (DAE 123) compared with Wet (DAE 137) during 1994 (Fig. 7b). Although g_s decreased throughout senescence (Fig. 7g, h), no C treatment inversion was observed (Fig. 7i, j). The precipitous drop in A that occurred during senescence (Fig. 7c, d, e, f) was greater for leaves grown at elevated compared with ambient C_a. In a companion study, Nie et al. (1995a, 1995b) showed a similar precipitous drop in total flag leaf and thylakoid polypeptide content, which can explain the rapid decline in A reported herein during senescence for leaves grown in elevated compared with ambient C_a (Fig. 7c, d, e, f). A rapid reduction in TNC also occurred during soft-dough (Fig. 8k) compared with that observed from tillering through milk-ripe (Fig. 8g, h, i, j). In open-top chambers maintained at 350, 525, and 750 μmol CO_2 mol^{-1}, Sicher and Bunce (1997) demonstrated that the effects of elevated C_a on total soluble and Rubisco protein content, chlorophyll content, and Rubisco activity of flag leaves of wheat and penultimate leaves of barley (*Hordeum vulgare* L.) were consistent with an acceleration of senescence. They concluded that the primary factor affecting Rubisco activity in response to elevated C_a was an acceleration in ontogeny that resulted in premature senescence. During the final 8 d of a 33-d experiment, that began before anthesis in wheat grown in open-top chambers maintained at 350 and 750 μmol CO_2 mol^{-1}, evidence of a premature senescence in flag leaf constituents (i.e., lower soluble protein, α-amino N, and chlorophyll *a* and *b* concentrations and higher acid proteinase activity) was observed in flag leaves grown in elevated compared with ambient C_a (Sicher and Bunce, 1998). Regardless of C_a treatment, plants grown in open-top-chamber studies had similar air turbulence and thermal regimes (±0.5°C). Consequently, the accelerated senescence observed by Sicher and Bunce (1998) was determined to be a direct consequence of elevated C_a rather than any artifact imposed by the open-top chamber itself. In a companion study, Pinter et al. (2000) attributed the accelerated senescence in flag leaves that reduced thylakoid polypeptide content for leaves reported by Nie et al. (1995a) and values of A reported herein (Fig. 6e, j; 7c, d, e, f) to the additional thermal energy caused by nighttime blower-induced turbulence in the C_a–enriched plots above and beyond that available in the ambient plots that had no blowers. Nevertheless, despite the presence or absence of blowers in the ambient plots, preanthesis photoassimilate was greater in elevated C_a plots because they had significant reductions in water stress–induced midafternoon depressions in carbon gain (Fig. 6). During senescence, however, a treatment inversion for A between elevated C_a and ambient plots occurred. An accelerated decline in photosynthetic capacity that reduced production of postanthesis photoassimilates in elevated C_a compared with ambient plants was first observed for water-stressed (Fig. 7e, f) compared with well-watered (Fig. 7c, d) plants. Based on values of A reported herein (Fig. 7c, d, e, f) and trends in green leaf area (Pinter et al., 1996), the accelerated senescence in leaves grown in elevated C_a is consistent with accelerated development and premature senescence reported elsewhere (Sionit et al., 1980a, 1980b; Morison and Gifford, 1984a, 1984b; Sicher and Bunce, 1998).

Carbohydrate Pool Dynamics

Hypothesis 7: Improved water relations that increase carbon gain will be evidenced by an increase in the TNC in source leaves

Throughout most of the growing season, the treatment response ranking for TNC was FW > CW ≅ FD > CD (Fig. 8a–d, g–j), but just before physiological maturity this treatment ranking nearly inverted to CD > FD > FW > CW (Fig. 8e–f, k). Overall, TNC levels were significantly greater during a year of mild water stress during 1993 (Fig. 8a–f), compared with a

year of more severe water stress during 1994 (Fig. 8g–k). Although the effect of FACE on TNC was nominal under Dry, it significantly increased TNC under Wet conditions (Fig. 8; Tables 1, 3).

During anthesis on DAE 89, 1994, when canopy height (Z) reached its maximum, TNC was measured for the flag through flag-4 leaves on individual culms (Fig. 9a). A significant Z effect ($P_\alpha \leq 0.0001$) occurred because TNC was significantly higher at the top of the canopy in the flag leaf and diminished thereafter from the flag-1 to flag-4 leaves (Fig. 9a). The TNC was higher in FACE compared with Control ($P_\alpha = 0.24$) for the flag through flag-3 leaves, but a significant $Z \times C$ interaction effect ($P_\alpha = 0.0001$) was observed because of a treatment inversion that occurred for the flag-4 leaf. Despite the overall seasonal and temporal trend for TNC levels to be higher in the upper-most sunlit leaf for Wet compared with Dry (Fig. 8), at anthesis on DAE 89 during 1994, significantly higher TNC levels were observed in Dry than Wet ($P_\alpha = 0.0009$) across the entire crop canopy. Nevertheless, a significant $Z \times I$ interaction effect ($P_\alpha = 0.0004$) occurred because this effect also diminished from the flag to the flag-4 leaves. Although the $C \times I$ interaction was insignificant ($P_\alpha = 0.82$), a pronounced $Z \times C \times I$ interaction effect ($P_\alpha = 0.15$) occurred because on a relative basis, a greater disparity in TNC levels occurred in leaves between CW and FW than between CD and FD, but this trend also diminished from the flag to the flag-4 leaves (Fig. 9b).

Because the export of simple sugars can lag behind production, accumulation of TNC in source leaves can cause physical manifestations such as discoloration, chlorosis, necrotic spots, brittleness, leaf curling, and even the onset of early senescence (Neales and Incoll, 1969; Mauney et al., 1979). Many of these visual signs of TNC accumulation, especially the onset of early senescence, were observed in the C_a–enriched plots (Fig. 7c, d, e, f). An abundance of preanthesis TNC production (Fig. 8) and decreased carboxylation capacity during senescence (Nie et al., 1995a), which diminished postanthesis TNC pools, suggest that during grain filling wheat plants grown in elevated C_a were more dependent on preanthesis and less reliant on postanthesis photoassimilate supply to reach physiological maturity. In a field study in Mexico, Bidinger et al. (1977) reported that preanthesis photosynthate supplied 0.12 and 0.22 of grain dry matter under well-watered and drought-stressed conditions, respectively. Gent (1994) reported that preanthesis TNC reserves contributed 0.20 to 0.50 of grain dry weight of winter wheat. More importantly, however, he reported that the contribution of TNC reserves to grain weight could be greater than 0.50 under

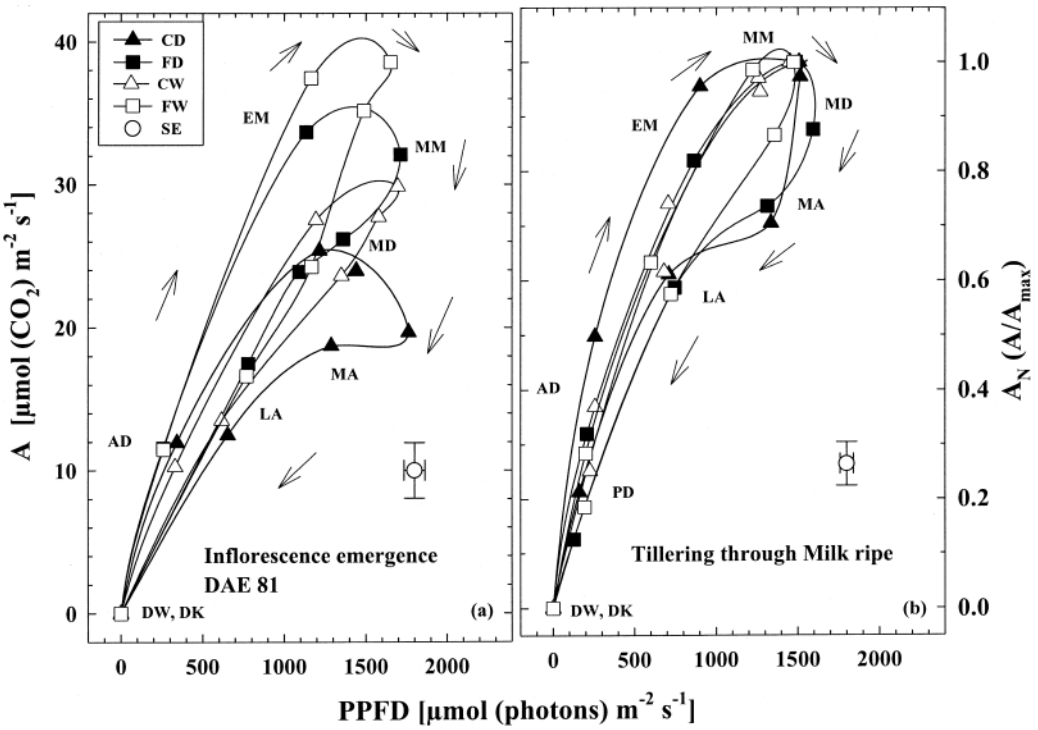

Fig. 10. Absolute mean leaf net assimilation rate (A) (left-most y axis) in response to diurnal course of incident photosynthetic photon flux density (PPFD) during inflorescence emergence on day after 50% emergence (DAE) 81 during the 1994 growing season (replotted from Fig. 6h). The season-long mean leaf net assimilation rate (A_N) was normalized to a relative scale between 0 and 1 by dividing each value of A, obtained per sample interval, by the daily maximum (A_{max}) leaf net assimilation rate (i.e., $A_N = A/A_{max}$) across all treatments, for both years, and all development stages except for soft and hard-dough (replotted from Fig. 6a–d and f–i). On the second y axis (right-most y axis), the resultant values of A_N were plotted in response to the diurnal course of (b) PPFD. Arrows denote direction of hysteresis loop from dawn (DW), after dawn (AD), early morning (EM), midmorning (MM), midday (MD), midafternoon (MA), late-afternoon (LA), predusk (PD), and dusk (DK). Symbol legend same as given in Fig. 1a. Open-circle symbol with two-way error bars denote the pooled SE across all sample intervals for the A (vertical) and PPFD (horizontal) parameters. The single diurnal course illustrated above in panel (a) was derived from measurements of as many as 360 leaves, whereas the normalized response was derived from measurements of as many as 3180 leaves.

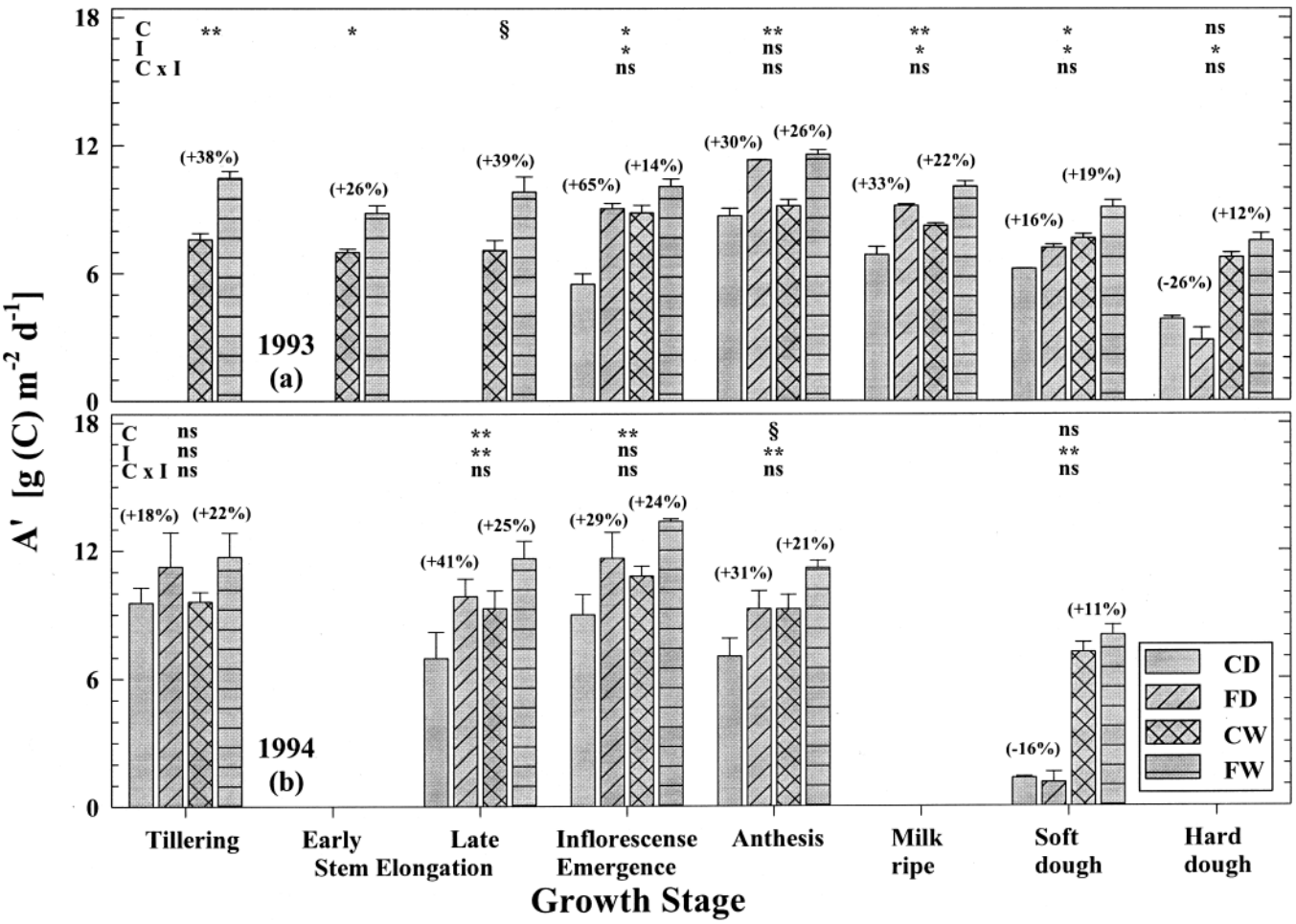

Fig. 11. Daily integrals of carbon accumulated (*A′*) for fully expanded sunlit spring wheat leaves at development stages given during the (a) 1993 and (b) 1994 growing seasons. (a) During 1993, eight measurement dates are shown for Wet (Garcia et al., 1998) and five for Dry. (b) During 1994, five sampling dates are shown for both Wet and Dry. Measurements were simultaneous with, and sampled as described for, *A* in Fig. 6. Symbols in legend, SE, percentages in parentheses, source of variance, and results from ANOVA same as described in Fig. 9. The above illustration was derived from measurements from as many as 3540 leaves.

stressful climates such as that reported herein for water-stressed wheat. Perhaps the amount of carbon accumulated in the kernels each day during grain filling was not as dependent on daily assimilation of carbon because preanthesis TNC reserves were greater in leaves grown in elevated compared with ambient C_a. Wechsung et al. (2000) demonstrated that under elevated C_a, the relative contribution of postanthesis photoassimilate of ears (i.e., awns and glumes) to grain filling was also reduced, presumably because higher levels of preanthesis TNC may have been translocated to the developing kernels.

Establishment of higher TNC pools during the sunlit period ensured that an adequate nocturnal carbon supply was available for growth and maintenance processes at night. During a year of mild water stress in 1993, the initial levels of TNC at dawn increased from the eighth leaf at stem elongation to flag leaf at anthesis (Fig. 8a–f), whereas during a year of more severe water stress during 1994 this trend was less prevalent (Fig. 8g–k). Nevertheless, this suggest that during 1993 (Fig. 5a–f), nocturnal consumption of TNC lagged behind the previous day's accumulation even during a period of rapid growth when TNC demand was high because of developing sinks such as shoots (Pinter et al., 1996) and roots (Wechsung et al., 1995, 1999) (Fig. 13). Since reserve TNCs in C_3 cool-season annual grasses, such as wheat, are normally stored in crown and sheath tissue (Weinmann, 1948), the presence of residual TNC during predawn in leaves following nocturnal consumption suggest that higher levels of reserves must have existed in organs known to store TNC (i.e., crown and leaf sheath). This suggests that throughout the season, elevated C_a may have caused daily net increases in TNC reserve pools. Consequently, we accept Hypothesis 7.

Growth and Yield Response

Hypothesis 8: Elevated C_a will foster a positive feedback relationship between aboveground source capacity (shoots) and belowground sink demand (roots), and this effect will be proportionately greater under dry than wet conditions

An increase in both WUE and IWUE, ample TNC pools and as much as a 1.5°C warmer uppermost canopy

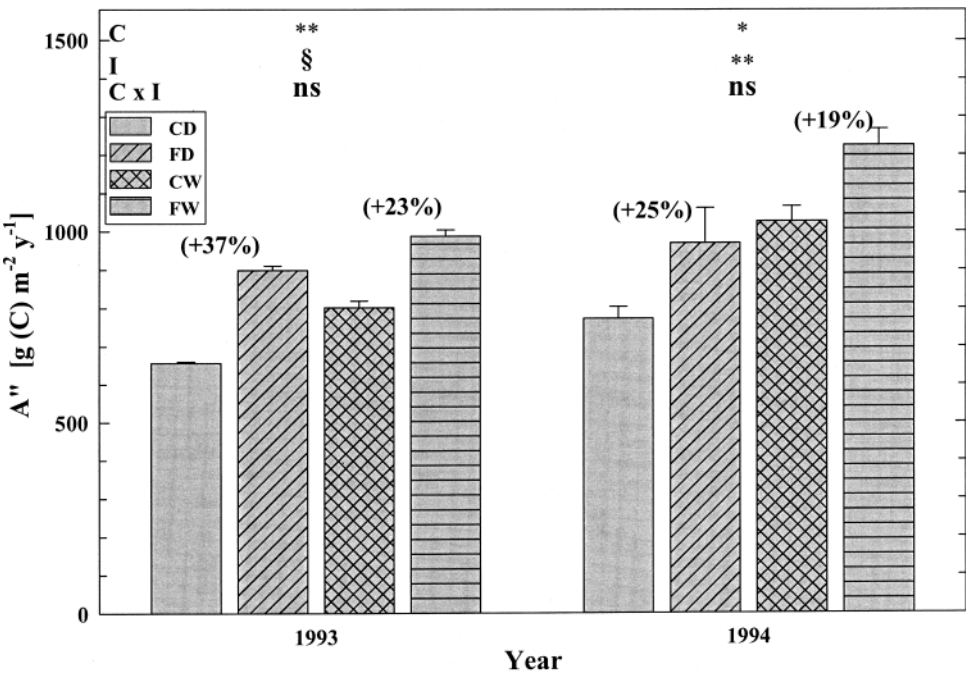

Fig. 12. Seasonal integral of total carbon accumulated (A'') (integration performed from 50% emergence until canopy senescence reduced fractional absorption of incident photosynthetically active radiation to 25%) for fully expanded sunlit spring wheat leaves during the 1993 and 1994 growing seasons. During 1993, A'' is based on eight measurement dates for Wet and Dry (i.e., $n = 8$). During 1994, A'' is based on five sampling dates for Wet and Dry (i.e., $n = 5$). Measurements were simultaneous with, and sampled as described for, A in Fig. 6. The SE, percentages in parentheses, symbols in legend, source of variance, and results from ANOVA same as described in Fig. 9. The above illustration was derived from as many as 3540 leaves.

sunlit leaf temperature reported herein (Table 3), and a0.6°C increase in whole-canopy temperature reported in a companion study (Kimball et al., 1995; Pinter et al., 2000), can explain the elevated C_a–induced increase in the initiation and growth of organs during seedling development (Li et al., 1997), an advantage that persisted throughout the remainder of the growing season (Kimball et al., 1995; Pinter et al., 1996). Elevated C_a caused an increase in A' (Fig. 11) and A'' (Fig. 12) carbon gain for uppermost sunlit leaves and also for those lower in the canopy (Fig. 9), which explains the 19 and 44% stimulation of whole-canopy net assimilation rate reported for well-watered and water-stressed wheat canopies, respectively (Kimball et al., 1995). Any C_a–induced enhancement in TNC reserves ensured that actual growth approximated that of potential (Li et al., 1997, 1999). It also ensured that any adaptation to drought (Turner and Long, 1980) that would require additional carbon supply was more likely to occur in water-stressed leaves grown in elevated C_a. An enhancement in drought adaptations because of elevated C_a (Wall, 2001; Wall et al., 2001a) minimized water loss and resulted in less negative Ψ_W (Fig. 3, 4, and 5), as observed in *Brassica* species (Uprety et al., 1995). An increase in TNC pools also enhanced morphological characteristics of roots that increased root mass (Fig. 13), length, density, and average thickness, thereby increasing root cylindrical surface area (Wall et al., 1996, 2001b; Wechsung et al., 1995, 1999)—particularly, for fine roots that are primarily responsible for absorption of water and nutrients. Therefore, it appears that the stimulation of carbon gain because of elevated C_a, mediated by an increase in TNC reserves, enabled a positive rather than a null or negative feedback between source capacity of aboveground (shoots) and belowground (roots) sinks (Diaz et al., 1993; Zak et al., 1993), and this effect was proportionately greater under Dry compared with Wet conditions. Hence, we accept Hypothesis 8.

Because there was an acceleration in senescence under elevated C_a—presumably because of ample supply of preanthesis photoassimilate-based TNC reserves and/or additional thermal energy provided by the blower-induced turbulence in the elevated C_a plots—the duration of grain filling was shortened in the FACE compared with Control plots (Li et al., 2000). Hence, the longer duration of the grain filling period for Control compared with FACE reduced the difference in grain yield between FACE and Control. Nevertheless, even though the postanthesis photoassimilate supply was reduced under elevated C_a, a consistently greater preanthesis TNC supply probably enhanced grain-filling rates (Li et al., 2000). Ultimately, elevated C_a resulted in an increased grain yield by 10 and 23% for well-watered and water-stressed wheat, respectively (Kimball et al., 1995; Pinter et al., 1996).

In view of these results, the accumulation of photoassimilates as TNC pools during the sunlit period, their utilization for growth and maintenance during the nocturnal period, and the quantity and location of long-term TNC storage reserves in plant organs is a subject of vital importance in global change research today, one that requires additional investigation.

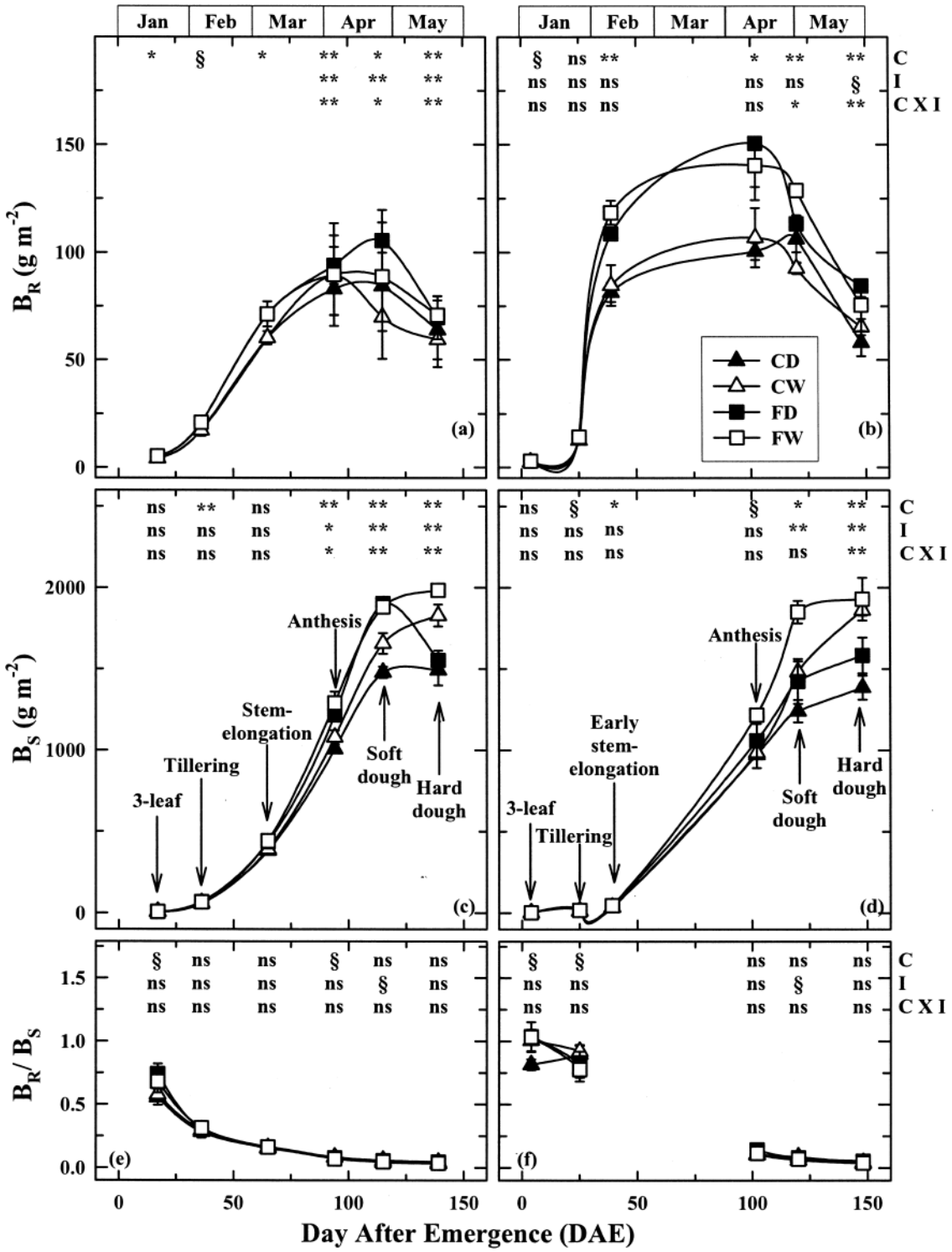

Fig. 13. Seasonal trend in the (a, b) total root biomass (B_R) in a 1-m soil profile and (c, d) shoot biomass (B_S), and (e, f) the root to shoot ratio (B_R/B_S) for spring wheat during the (a, c, e) 1993 and (b, d, f) 1994 growing seasons. Sampling occurred on day after emergence (DAE) 16 and DAE 3 at the 3-leaf, DAE 36 and DAE 26 at tillering, DAE 63 and DAE 40 at stem-elongation, DAE 92 and DAE 102 at anthesis, DAE 113 and 118 at soft dough, and DAE 159 and DAE 154 at hard dough developmental stages during the 1993 and 1994 growing seasons, respectively. Each mean datum for B_R was derived from four replications during vegetative development (i.e., 3-leaf, tillering, stem-elongation) and two replications during reproductive development (i.e., anthesis, soft dough, hard dough) (i.e., means and SE of replication means based on $n = 4$ and $n = 2$, respectively). During 1994, the B_R was collected for four replications during vegetative and three replications during reproductive development (i.e., means and SE of replication means based on $n = 4$ and $n = 3$, respectively). The total B_S (i.e., aboveground green and brown leaves, sheaths, culms and ears, and belowground crown tissue) was collected for four replications both seasons (i.e., means based on $n = 4$, SE of replication means based on $n = 4$). Symbols in legend, source of variance, and results from ANOVA same as described in Fig. 1.

CONCLUSIONS

Our results demonstrate that elevated C_a reduced the deleterious effects of water stress on wheat by increasing both drought avoidance (i.e., decrease in g_s and TR coupled with a more robust fine root system to absorb water and nutrients) and drought tolerance (i.e., an increase in seasonal carbon gain that enhanced osmoregulation and acclimation of tissue to drought) mechanisms. Hence, in the absence of any adverse effects of a concomitant rise in global temperature resulting from the rise in C_a, improved water relations for a herbaceous, cool-season, annual, C_3 cereal monocot grass (i.e., wheat) are anticipated in the future high-CO_2 world. Improved water relations will reduce water stress–induced midafternoon depressions in A, thereby increasing A' and A''. Improved water status and carbon pool dynamics will result in an elevated C_a–based increase in above- and belowground growth. Hence, despite any water stress–based constraints, a rise in C_a will reduce the deleterious effects of drought on physiological processes. Results reported herein are applicable in the assessment of productivity of other graminaceous species of a similar function-type as wheat common to temperate zone grassland prairies and savannas, especially under dryland conditions.

ACKNOWLEDGMENTS

This research was supported by the Agricultural Research Service, USDA, including the U.S. Water Conservation Laboratory, Phoenix, AZ; the Grassland Soil and Water Research Laboratory, Temple, TX; and the Plant Stress and Protection Group, Gainesville, FL. Operational support was also contributed by the Potsdam Institute for Climate Impact Research, Potsdam, Germany; by the NASA Goddard Space Flight Center, Greenbelt, MD; by the Natural Resource Ecology Laboratory, Colorado State University, Ft. Collins, CO; by the Department of Soil Science, University of Alberta, Edmonton, AB, Canada; and by Grant IBN-9652614 from the NSF-DOE-NASA-USDA Joint Program on Terrestrial Ecology and Global Change (TECO II) to the Agricultural Research Service, USDA, U.S. Water Conservation Laboratory, Phoenix, AZ (Gerard W. Wall, PI). We also acknowledge the helpful cooperation of Dr. Roy Rauschkolb (deceased) and his staff at the Maricopa Agricultural Center. The FACE apparatus was furnished by Brookhaven National Laboratory, and we are grateful to Mr. Keith Lewin, Dr. John Nagy, and Dr. George Hendrey for assisting in its installation and consulting about its use. This work contributes to the Global Change Terrestrial Ecosystem (GCTE) Core Research Programme, which is part of the International Geosphere–Biosphere Programme (IGBP). Technical assistance of Ms. Laura M. Olivieri who prepared the figures is appreciated.

REFERENCES

Acevedo, E., E. Fereres, T.C. Hsiao, and D.W. Henderson. 1979. Growth trends, water potential and osmotic adjustment of maize and sorghum leaves in the field. Plant Physiol. 64:476–480.

Ainsworth, E.A., and S.P. Long. 2005. What have we learned from 15 years of free-air CO_2 enrichmernt (FACE)? A meta-analytic review of the responses of photosynthesis, canopy properties and plant production to rising CO_2. New Phytol. 165:351–372.

Allen, L.H., R.R. Valle, J.W. Jones, and P.H. Jones. 1998. Soybean leaf water potential responses to carbon dioxide and drought. Agron. J. 90:375–383.

Azcón-Bieto, J. 1983. Inhibition of photosynthesis by carbohydrates in wheat leaves. Plant Physiol. 73:681–686.

Bennett, J.M., P.M. Cortes, and F.G. Lorens. 1986. Comparison of water potential components measured with a thermocouple psychrometer and a pressure chamber and the effects of starch hydrolysis. Agron. J. 78:239–244.

Bidinger, F., R.B. Musgrave, and R.A. Fischer. 1977. Contribution of stored preanthesis assimilate to grain yield in wheat and barley. Nature (London) 270:431–433.

Blum, A., J. Mayer, and G. Golan. 1988. The effect of grain number per ear (sink size) on source activity and its water relations in wheat. J. Exp. Bot. 46:233–235.

Box, G.E.P., W.G. Hunter, and J.S. Hunter. 1978. Statistics for experimenters: An introduction to design, data analysis, and model building. John Wiley & Sons, New York.

Boyer, J.S. 1971. Recovery of photosynthesis in sunflower after a period of low leaf water potential. Plant Physiol. 47:816–820.

Briscoe, R.D. 1984. Thermocouple psychrometers for water potential measurements. p. 1–14. *In* Proc. of the NATO Advanced Study Institute on Advanced Agricultural Instrumentation, II Ciocco (Pisa), Italy. 27 May–9 June 1984.

Brown, R.W., and J.M. Collins. 1980. A screen-caged thermocouple psychrometer and calibration chamber for measurements of plant and soil water potential. Agron. J. 72:851–854.

Campbell, G.S., R.I. Papendick, E. Rabie, and A.J. Shayo-Ngowi. 1979. A comparison of osmotic potential, elastic modulus, and apoplastic water in leaves of dryland wheat. Agron. J. 71:31–36.

Chatterton, N.J., P.A. Harrison, J.H. Bennet, and W.R. Thornley. 1987. Fructans, starch and sucrose concentrations in crested wheatgrass and redtop as affected by temperature. Plant Physiol. Biochem. 25:617–623.

DeLucia, E.H., T.W. Sasek, and B.R. Strain. 1985. Photosynthetic inhibition after long-term exposure to elevated levels of atmospheric carbon dioxide. Photosynth. Res. 7:175–184.

Denmead, O.T., and B.D. Millar. 1976. Water transport in wheat plants in the field. Agron. J. 68:297–303.

Diaz, S., J.P. Grime, J. Harris, and E. McPherson. 1993. Evidence of a feedback mechanism limiting plant response to elevated carbon dioxide. Nature (London) 364:616–617.

Doorenbos, J., and W.O. Pruitt. 1977. Crop water requirements. Irrig. and Drain. Pap. 24. FAO, Rome, Italy.

Drake, B.G., M.A. Gonzalez-Meler, and S.P. Long. 1997. More efficient plants? A consequence of rising atmospheric CO_2. Annu. Rev. Plant Physiol. Plant Mol. Biol. 48:607–637.

Estiarte, M., J. Penuelas, B.A. Kimball, S.B. Idso, R.L. LaMorte, P.J. Pinter, Jr., G.W. Wall, and R.L. Garcia. 1994. Elevated CO_2 effects on stomatal density of wheat and sour orange trees. J. Exp. Bot. 45:1665–1668.

Farquhar, G.D., and T.D. Sharkey. 1982. Stomatal conductance and photosynthesis. Annu. Rev. Plant Physiol. 33:317–345.

FAO, Food and Agriculture Organization of the United Nations. 1996. *In* Statistical databases FAO. Available at www.fao.org (accessed 20 May 2005; verified 1 Oct. 2005). FAO, Rome, Italy.

Fox, F.A., Jr., T. Scherer, D.C. Slack, and L.J. Clark. 1992. AriZona irrigation SCHEDuling user's manual. Coop. Ext., Agric., and Biosyst. Eng., Univ. of Arizona, Tucson, AZ.

Foyer, C.H. 1988. Feedback inhibition of photosynthesis through source–sink regulation in leaves. Plant Physiol. Biochem. 26:483–492.

Garcia, R.L., S.P. Long, G.W. Wall, C.P. Osborne, B.A. Kimball, G.Y. Nie, P.J. Pinter, Jr., R.L. LaMorte, and F. Wechsung. 1998. Photosynthesis and conductance of spring-wheat leaves: Field response to continuous free-air atmospheric CO_2 enrichment. Plant Cell Environ. 21:659–669.

Gent, M.P.N. 1994. Photosynthate reserves during grain filling in winter wheat. Agron. J. 86:159–167.

Hendrey, G.R. 1993. FACE: Free-air CO_2 enrichment for plant research in the field. CRC Press, Boca Raton, FL.

Hendrix, D.L. 1992. Influence of elevated CO_2 on leaf starch of field-grown cotton. p. 223–226. *In* G.R. Hendrey (ed.) FACE: Free-air CO_2 enrichment for plant research in the field. CRC Press, Boca Raton, FL.

Hendrix, D.L. 1993. Rapid extraction and analysis of nonstructural carbohydrates in plant tissues. Crop Sci. 33:1306–1311.

Hendrix, D.L., J.R. Mauney, B.A. Kimball, K.F. Lewin, J. Nagy, and G.R. Hendrey. 1994. Influence of elevated CO_2 and mild water stress on nonstructural carbohydrates in field-grown cotton tissues. Agric. For. Meteorol. 70:153–162.

Hendrix, D.L., and K.K. Peelen. 1987. Artifacts in the analysis of plant tissue for soluble carbohydrates. Crop Sci. 27:710–715.

Hunsaker, D.J., B.A. Kimball, P.J. Pinter, Jr., R.L. LaMorte, and G.W. Wall. 1996. Carbon dioxide enrichment and irrigation effects on wheat evapotranspiration and water use efficiency. Trans. ASAE 39:1345–1355.

IPCC, Intergovernmental Panel on Climate Change. 1996. Climate change 1995: Summary for policy makers. p. 1–7. *In* J.T. Houghton et al. (ed.) Cambridge Univ. Press, Cambridge, New York.

IPCC, Intergovernmental Panel on Climate Change. 2001. Climate change 2001: The scientific basis—contribution of working group I to the third assessment report of the Intergovernmental Panel of Climate Change. Cambridge Univ. Press, Cambridge, New York.

Jensen, M.E., R.D. Burman, and R.G. Allen. 1990. Evapotranspiration and irrigation water requirements. Am. Soc. of Civil Eng., New York.

Johnson, R.C., H.T. Nguyen, and L.I. Croy. 1984. Osmotic adjustment in two wheat genotypes differing in drought resistance. Crop Sci. 24:957–962.

Kameli, A., and D.M. Losel. 1994. Contribution of carbohydrates and other solutes to osmotic adjustment in wheat leaves under water stress. J. Plant Physiol. 145:363–366.

Kimball, B.A., R.L. LaMorte, P.J. Pinter, Jr., G.W. Wall, D.J. Hunsaker, F.J. Adamsen, S.W. Leavitt, T.L. Thompson, A.D. Matthias, and T.J. Brooks. 1999. Free-Air CO_2 Enrichment (FACE) and soil nitrogen effects on energy balance and evapotranspiration of wheat. Water Resour. Res. 35:1179–1190.

Kimball, B.A., P.J. Pinter, Jr., R.L. Garcia, R.L. LaMorte, G.W. Wall, D.J. Hunsaker, G. Wechsung, F. Wechsung, and T. Kartschall. 1995. Productivity and water use of wheat under free-air CO_2 enrichment. Global Change Bio. 1:429–442.

Kirkham, M.B. 1990. Plant responses to water deficits. p. 323–342. *In* B.A. Stewart and D.R. Nielsen (ed.) Irrigation of agricultural crops. Agron. Monogr. 30. ASA, CSSA, and SSSA, Madison, WI.

Krapp, A., B. Hoffmann, C. Fer, and M. Stitt. 1993. Regulation of the expression of the rbcS and other photosynthetic genes by carbohydrates: A mechanism for the "sink regulation" of photosynthesis? Plant J. 3:817–828.

Krapp, A., P. Quick, and M. Stitt. 1991. Ribulose-1,5-bisphosphate carboxylase-oxygenase, other Calvin-cycle enzymes, and clorophyll decrease when glucose is supplied to mature spinach leaves via the transpiration stream. Planta 186:58–69.

Li, A.G., Y.S. Hou, G.W. Wall, A. Trent, B.A. Kimball, and P.J. Pinter, Jr. 2000. Free air CO_2 enrichment and drought stress effects on grain filling rate and duration in spring wheat. Crop Sci. 40:1263–1270.

Li, A.G., A. Trent, G.W. Wall, B.A. Kimball, Y.S. Hou, P.J. Pinter, Jr., R.L. Garcia, D.J. Hunsaker, and R.L. LaMorte. 1997. Free-air CO_2 enrichment effects on rate and duration of apical development of sping wheat. Crop Sci. 37:789–796.

Li, A.G., G.W. Wall, A. Trent, and Y.S. Hou. 1999. Free-air CO_2 enrichment effects on apex dimensional growth of spring wheat. Crop Sci. 39:1083–1088.

LI-COR. 1990. LI–COR technical reference. LI–COR, Lincoln, NE.

Littell, R.C., G.A. Milliken, W.W. Stroup, and R.D. Wolfinger. 1996. SAS system for mixed models. SAS Inst., Cary, NC.

Long, S.P., E.A. Ainsworth, A. Rogers, and D.R. Ort. 2004. Rising atmospheric carbon dioxide: Plants Face the future. Annu. Rev. Plant Biol. 55:591–628.

Mauney, J.R., G. Guinn, K.E. Fry, and J.D. Hesketh. 1979. Correlation of photosynthetic carbon dioxide uptake and carbohydrate accumulation of cotton, soybean sunflower and sorghum. Photosynthetetica 13:260–266.

McCarthy, J.J., O.F. Canziani, N.A. Leary, and D.J. Dokken. 2001. K.S. White (ed.) Climate change 2001: Impacts, Adaptation and Vulnerability, Contribution of Working Group II to the Third Assessment Report of the Intergovernmental Panel on Climate Change. Cambridge Univ. Press, Cambridge, UK.

Millar, B.D., and O.T. Denmead. 1976. Water relations of wheat leaves in the field. Agron. J. 68:303–307.

Morgan, J.M. 1980a. Osmotic adjustment in the spikelets and leaves of wheat. Environ. Exp. Bot. 31:655–665.

Morgan, J.M. 1980b. Osmotic components and properties associated with genotypic differences in osmoregulation in wheat. Austr. J. Plant Physiol. 19:67–76.

Morgan, J.M., and A.G. Condon. 1986. Water use, grain yield, and osmoregulation in wheat. Aust. J. Plant Physiol. 13:523–532.

Morison, J.I.L. 1993. Response of plants to CO_2 under water limited conditions. Vegetatio 104/105:193–209.

Morison, J.I.L. 1998. Stomatal response to increased CO_2 concentration. J. Exp. Bot. 49:443–452.

Morison, J.I.L., and R.M. Gifford. 1984a. Plant growth and water use with limited water supply in high CO_2 concentrations: I. Leaf area, wateruse and transpiration. Aust. J. Plant Physiol. 11:361–374.

Morison, J.I.L., and R.M. Gifford. 1984b. Plant growth and water use with limited water supply in high CO_2 concentrations: II. Plant dry weight, partitioning and water use efficiency. Aust. J. Plant Physiol. 11:375–384.

Munns, R., C.J. Brady, and E.W.R. Barlow. 1979. Solute accumulation in the apex and leaves of wheat during water stress. Aust. J. Plant Physiol. 6:379–389.

Munns, R., and R. Weir. 1981. Contribution of sugars to osmotic adjustment in elongating and expanded zones of wheat leaves during moderate water deficits at two light levels. Aust. J. Plant Physiol. 8:93–105.

Neales, T.F., and I.D. Incoll. 1969. The control of leaf photosynthesis rate by the level of assimilate concentration in the leaf: A review of the hypothesis. Bot. Rev. 34:107–125.

Nie, G.Y., D.L. Hendrix, A.N. Webber, B.A. Kimball, and S.P. Long. 1995a. Increased accumulation of carbohydrates and decreased photosynthetic gene transcript levels in wheat grown at an elevated CO_2 concentration in the field. Plant Physiol. 108: 975–983.

Nie, G.Y., S.P. Long, R.L. Garcia, B.A. Kimball, R.L. LaMorte, P.J. Pinter, Jr., G.W. Wall, and A.N. Webber. 1995b. Effects of free-air CO_2 enrichment on the development of the photosynthetic apparatus in wheat, as indicated by changes in leaf proteins. Plant Cell Environ. 18:855–864.

Pinter, P.J., Jr., B.A. Kimball, R.L. Garcia, G.W. Wall, D.J. Hunsaker, and R.L. LaMorte. 1996. Free-air CO_2 enrichment: Responses of cotton and wheat crops. p. 215–249. *In* G.W. Koch and H.A. Mooney (ed.) Carbon dioxide and terrestrial ecosystems. Academic Press, San Diego, CA.

Pinter, P.J., Jr., B.A. Kimball, G.W. Wall, R.L. LaMorte, D.J. Hunsaker, F.J. Adamsen, K.F.A. Frumau, H.F. Vugts, G.R. Hendrey, K.F. Lewin, J. Nagy, H.B. Johnson, F. Wechsung, S.W. Leavitt, T.L. Thompson, A.D. Matthias, and T.J. Brooks. 2000. Free-Air CO_2 Enrichment (FACE): Blower effects on wheat canopy microclimate and plant development. Agric. For. Meteorol. 103:319–333.

Pollock, C.J. 1986. Fructans and the metabolism of sucrose in vascular plants. New Phytol. 104:1–24.

Post, D.F., C. Mack, P.D. Camp, and A.S. Sulliman. 1988. Mapping and characterization of the soils on the University of Arizona, Maricopa Agricultural Center. Proc. Hydrol. Water Resour. 18:49–60.

Robertson, M.J., S. Fukai, M.M. Ludlow, and G.L. Hammer. 1993a. Water extraction by grain sorghum in a sub humid environment: I. Analysis of the water extraction pattern. Field Crops Res. 33: 81–97.

Robertson, M.J., S. Fukai, M.M. Ludlow, and G.L. Hammer. 1993b. Water extraction by grain sorghum in a sub humid environment: II. Extraction in relation to root growth. Field Crops Res. 33:99–112.

Samarakoon, A.B., and R.M. Gifford. 1995. Soil water content under plants at high CO_2 concentration and interactions with the direct CO_2 effects: A species comparison. J. Biogeo. 22:193–202.

Scholander, P.F., H.T. Hammel, E.D. Bradstreet, and E.A. Hemmingsen. 1965. Sap pressure in vascular plants. Science (Washington, DC) 148:339–346.

Senock, R.S., J.M. Ham, T.M. Loughin, B.A. Kimball, D.J. Hunsaker, P.J. Pinter, Jr., G.W. Wall, R.L. Garcia, and R.L. LaMorte. 1996. Sap flow in wheat under free-air CO_2 enrichment. Plant Cell Environ. 19:147–158.

Sharkey, T.D., and J.R. Seemann. 1989. Mild water stress effects on carbon-reduction-cycle intermediates, ribulose biphosphate carboxylase activity, and spacial homogeneity of photosynthesis in intact leaves. Plant Physiol. 89:1060–1065.

Sicher, R.C., and J.A. Bunce. 1997. Relationship of photosynthetic acclimation to changes of Rubisco activity in field-grown winter wheat and barley during growth in elevated carbon dioxide. Photosynth. Res. 52:27–38.

Sicher, R.C., and J.A. Bunce. 1998. Evidence that premature senescence affects photosynthetic decline of wheat flag leaves during growth in elevated carbon dioxide. Int. J. Plant Sci. 159:789–804.

Sionit, N., H. Hellmers, and B.R. Strain. 1980a. Growth and yield of wheat under CO_2 enrichment and water stress. Crop Sci. 20:687–691.

Sionit, N., I.D. Teare, and P.J. Kramer. 1980b. Effects of repeated application of water stress on water status and growth of wheat. Physiol. Plant. 50:11–15.

Sionit, N., B.R. Strain, and H. Hellmers. 1981a. Effects of different concentrations of atmospheric CO_2 on growth and yield components of wheat. J. Agric. Sci. Camb. 79:335–339.

Sionit, N., B.R. Strain, H. Hellmers, and P.J. Kramer. 1981b. Effects of atmospheric CO_2 concentration and water stress on water relations of wheat. Bot. Gaz. 142:191–196.

Smucker, A.J.M., S.L. McBurney, and A.K. Srivastava. 1982. Quantitave separation of roots from compacted soil profiles by the hydropneumatic elutiation system. Agron. J. 74:500–503.

Steffen, W.L., B.H. Walker, J.S. Ingram, and G.W. Koch. 1992. The operational plan. Rep. 21. International Geosphere–Giosphere Programme, Global Change and Terrestrial Ecosystems. International Council of Scientific Unions, Stockholm, Sweden.

Stitt, M. 1991. Rising CO_2 levels and their potential significance for carbon flow in photosynthetic cells. Plant Cell Environ. 14: 741–762.

Tenhunen, J.D. 1984. Changes in photosynthetic capacity, carboxylation efficiency and CO_2 compensation point associated with midday stomatal closure and midday depression of net CO_2 exchange of leaves of *Quercus suber*. Planta 162:193–203.

Tenhunen, J.D., O.L. Lange, M. Braun, A. Meyer, R. Losch, and J.S. Pereira. 1980. Midday stomatal closure in *Arbutus unedo* leaves in a natural macchia and under simulated habitat conditions in an environmental chamber. Oecologia 472:1–3.

Turner, N.C., and M.J. Long. 1980. Adaptation of plants to water and high temperature stress. John Wiley & Sons, New York.

Turner, N.C., and M.J. Long. 1990. Errors arising from rapid water loss in the measurement of leaf water potential by the pressure chamber technique. Aust. J. Plant Physiol. 7:527–537.

Uprety, D.C., R.S. Mishra, and Y.P. Abrol. 1995. Effect of elevated CO_2 on the photosynthesis, growth and water relation of *Brassica* species under moisture stress. J. Agron. Crop Sci. 175:231–237.

von Caemmerer, S., and G.D. Farquhar. 1981. Some relationships between the biochemistry of photosynthesis and the gas exchange of leaves. Planta 153:376–387.

von Caemmerer, S., and G.D. Farquhar. 1984. Effects of partial defoliation, changes in irradiance during growth, short-term water stress and growth at enhanced (CO_2) on photosynthetic capacity of leaves of *Phaseolus vulgaris*. Planta 160:320–329.

Walker, S., D.M. Oosterhuis, and M.J. Savage. 1983. Field use of screen caged thermocouple psychrometers in sample chambers. Crop Sci. 23:627–632.

Wall, G.W. 2000. Simple filtration system improves efficiency of a hydropneumatic root elutriator. Commun. Soil Sci. Plant Anal. 31:975–980.

Wall, G.W. 2001. Elevated atmospheric CO_2 alleviates drought stress in wheat. Agric. Ecosyst. Environ. 1756:1–11.

Wall, G.W., N.R. Adam, T.J. Brooks, B.A. Kimball, P.J. Pinter, Jr., R.L. LaMorte, F.J. Adamsen, D.J. Hunsaker, G. Wechsung, F. Wechsung, S. Grossman-Clarke, S.W. Leavitt, A.D. Matthias, and A.N. Webber. 2000. Acclimation response of spring wheat in a Free-Air CO_2 Enrichment (FACE) atmosphere with variable soil nitrogen regimes: II. Net assimilation and stomatal conductance of leaves. Photosynth. Res. 66:79–95.

Wall, G.W., T.J. Brooks, N.R. Adam, A. Cousins, B.A. Kimball, P.J. Pinter, Jr., R.L. LaMorte, J. Triggs, M.J. Ottman, S.W. Leavitt, A.D. Matthias, D.G. Williams, and A.N. Webber. 2001a. Elevated atmospheric CO_2 improved sorghum plant water status by ameliorating the adverse affects of drought. New Phytol. 152:231–248.

Wall, G.W., R.L. Garcia, B.A. Kimball, P.J. Pinter, Jr., and R.L. Lamorte. 1996. Effects of free-air CO_2 enrichment and variable soil moisture regimes on root parameters of spring wheat. p. 56–59. *In* Annual research report. U.S. Water Conserv. Lab., USDA-ARS, Phoenix, AZ.

Wall, G.W., and B.A. Kimball. 1993. Biological databases derived from free-air carbon dioxide enrichment experiments. p. 329–351. *In* E.D. Schulze and H.A. Mooney (ed.) Design and execution of experiments on CO_2 enrichment. Environmental Research Programme, Commission of the European Communities, Brussels, Belgium.

Wall, G.W., B.A. Kimball, F.J. Adamsen, P.J. Pinter, Jr., F. Wechsung, Th. Kartschall, and S.W. Leavitt. 2001b. Elevated atmospheric carbon dioxide affects root dimensions of spring wheat. *In* Annual meetings abstracts [CD-ROM]. ASA, CSSA, and SSSA, Madison, WI.

Wechsung, F., R.L. Garcia, G.W. Wall, T. Kartschall, B.A. Kimball, P. Michaelis, P.J. Pinter, Jr., G. Wechsung, S. Grossman-Clarke, R.L. LaMorte, F.J. Adamsen, S.W. Leavitt, T.L. Thompson, A.D. Matthias, and T.J. Brooks. 2000. Photosynthesis and conductance of spring wheat ears: Field response to free-air CO_2 enrichment and limitation in water and nitrogen supply. Plant Cell Environ. 23:917–929.

Wechsung, G., F. Wechsung, G.W. Wall, F.J. Adamsen, B.A. Kimball, R.L. Garcia, P.J. Pinter, Jr., and Th. Kartschall. 1995. Biomass and growth rate of a spring wheat root system grown in Free-Air CO_2 Enrichment (FACE) and ample soil moisture. J. Biogeo. 22: 623–634.

Wechsung, G., F. Wechsung, G.W. Wall, F.J. Adamsen, B.A. Kimball, P.J. Pinter, Jr., R.L. LaMorte, R.L. Garcia, and Th. Kartschall. 1999. The effects of free-air CO_2 enrichment and soil water availability on spatial and seasonal patterns of wheat root growth. Global Change Bio. 5:519–529.

Weinmann, H. 1948. Underground development and reserves of grasses: A review. J. Br. Grassl. Soc. 3:115–140.

Wullschleger, S.D., T.J. Tschaplinski, and R.J. Norby. 2002. Plant water relations at elevated CO_2–implications for water-limited conditions. Plant Cell Environ. 25:319–331.

Zadoks, J.C., T.T. Chang, and C.F. Konzak. 1974. A decimal code for the growth stages of cereals. Weed Res. 14:415–421.

Zak, D.R., K.S. Pregitzer, P.S. Curtis, J.A. Terri, R. Fogel, and D.L. Randlett. 1993. Elevated atmospheric carbon dioxide and feedback between carbon and nitrogen cycles. Plant Soil 151:105–117.